I-B MODELING OF FISCHER TROPSCH REACTORS

by

Awdhoot V. Kerkar

and

Yatish T. Shah

Chemical and Petroleum Engineering Department
University of Pittsburgh
Pittsburgh, PA 15261

CONTENTS

LIST OF FIGURES

LIST OF FIGURES (Continued)

LIST OF TABLES

SUMMARY

This section deals with the modeling of performance of reactors used for Fischer-Tropsch Synthesis. The reactors include, bubble column slurry reactor, fluidized bed reactor and fixed bed reactor.

Based on the study of various kinetic expressions suggested in literature of Fischer-Tropsch synthesis over conventional catalysts such as Fe, Co, Ni, Ru, a first order and a power law type kinetic expression have been chosen. Computer programs incorporating the operational and design features of each of the reactor types have been developed. Each program is written in a modular form using FORTRAN language and in a manner such that, the user could update any part of it with ease.

The use of these simulators requires the design parameters, operating conditions and kinetic parameters to be supplied by the user. This is achieved via interactive programs which have to be executed prior to the main programs. Certain inherent physico-chemical and operational properties pertinent to each of the reactors are evaluated from correlations reported in literature. On execution, the main program gives the syngas conversion and the concentration of the various species along the reactor axis. These programs can be used to study the effect of various operating and design parameters on the reactor performance.

Comparison of reactor performance based on the conversion obtainable and the space time yield under identical operating conditions can also be made using these simulators.

Introduction

As early as 1902 it was observed that methane was formed from mixtures of H_2 and CO over nickel, and cobalt catalysts. (Sabatier and Senderens, 1902). In 1923 Fischer and Tropsch reported their work using alkalized iron catalyst at high pressure (Fischer and Tropsch, 1923) and this route of hydrogenation of carbon monoxide to form saturated and unsaturated compounds of the homologous hydrocarbon series became known as the Fischer Tropsch (F-T) synthesis.

This route permits the synthesis of hydrocarbons ranging from methane to high-melting paraffins with molecular weights above 20,000, depending on the catalyst, temperature and type of process employed. By-products such as alcohols, aldehydes, ketones, acids and esters are formed on a smaller scale. Small amounts of aromatic compounds are also formed at high temperature.

The F-T synthesis can be reduced to three fundamental reactions: viz. the hydrogenation of carbon monoxide and the conversion of water, commonly referred to, as the water-gas shift reaction,

$$(2n+1)H_2+nCO \rightarrow C_nH_{2n+2}+nH_2O$$

$$2nH_2+nCO \rightarrow C_nH_{2n}+nH_2O$$

$$CO + H_2O \quad H_2 + CO$$

Hydrocarbons can also be obtained via CO_2 formation. The olefin content of the synthesis product lies between 0 and 90% varying considerably with the chain length and the type of process. Undesirable side reactions, such as, hydrogenation of CO to methane, decomposition of CO to carbon and CO_2, and oxidation of catalyst are also observed and seriously hamper the hydrocarbon

synthesis. Thus, the hydrogenation of carbon monoxide according to the F-T process represents a complex system of parallel and consecutive reactions. Even though it was discovered in 1926, the reaction mechanism of the F-T synthesis has not yet been fully explained. Even the micro-kinetics of the F-T reaction are not known in their individual steps. Calculation of the simultaneous thermodynamic equilibria can be made only under certain simplying assumptions. A treatment of the thermodynamics of the F-T reaction including all the reactions involved in the synthesis, but assumed to take place independently of each other, was published by Anderson. (Anderson and Emmett, 1952).

Besides the complexity of the reaction mechanism, the major technical problems involved in the F-T synthesis include a rapid removal of heat of reaction, avoiding local overheating of the catalyst, which favors methane formation; and finally, a uniform distribution of synthesis gas over the catalyst. To solve these problems, various types of synthesis reactors have been developed. (Frohning et al. 1977). These reactors may be classified into those with stationary catalysts (lamellar reactor, double tube reactor, ARGE reactor) and those with mobile catalysts (fluidized-bed reactor, entrained bed reactor, three-phase slurry reactor).

The technology of manufacture of hydrocarbons via the Fischer-Tropsch synthesis was first employed by the Germans during the World War. In 1936, the first four F-T productions plants were commisioned and had a total capacity of 200,000 tons of hydrocarbon per year (Frohning et al., 1977). By 1944, the potential capacity of the nine plants in Germany was about 700,000 tons per year. After the war the two German firms, Rhurchemie and Lurgi, in a collaborative effort developed the ARGE fixed bed reactor. Work was also underway in the US (e.g. Standard Oil and Hydrogenation Research, Inc.), on

the F-T synthesis. The Kellogg Co. developed a circulating entrained catalyst version of a fluidized bed reactor which produced high yields of gasoline. The first commercial venture of the F-T process was commisioned in 1955 at Sasol, in South Africa. Both, the fixed bed Arge reactors and the entrained bed Kellogg reactors, are used for the synthesis. After numerous modifications, both in the operational and the mechanical aspects, the two systems have been successfully geared into a highly reliable large scale commercial operation.

Up to and during the second World War, the major research effort in Fischer-Tropsch synthesis was carried out in Germany with some research activity in USA during the post war period, but with the discovery of large oil deposits in the Middle East during the mid 1950's, interest in the F-T synthesis waned. It was only after 1973, due to the sudden oil embargo in the Middle East that there has been a resurgence of interest in the F-T process and a lot of money and technical knowhow has been diverted towards research in F-T synthesis. This recent trend can be well appreciated from the number of publications and reviews appearing in technical literature.

In the present work, mathematical models describing the F-T synthesis in a bubble column slurry reactor, a fluidized bed reactor and a fixed bed reactor have been developed.

Following is a detailed report on the model equations for each of the reactor types, along with the assumptions, the correlations used for the estimation of physico-chemical properties pertinent to each reactor, the

development of the computer programs, a detailed user's manual for an easy access to the programs and the results obtained thereof.

Every computer program is made modular, so that the user can modify any part of it, as and when required. The possible modifications include, updating correlations for physiochemical and hydrodynamic properties pertinent to the system and the kinetic expressions; although changes in the latter would call for major changes in the computer programs. The programs could be used for studying the effects of various operating and design parameters on the reactor performance.

Slurry Bubble Column Reactor

The use of slurry bubble column reactors in varied chemical processes such as chlorination, oxidation and fermentation has had considerable success, due to the favorable mixing and mass transfer properties combined with low shear stressing of the biological material. Recently, considerable interest has grown in understanding the operation of these reactors, because of their application in coal conversion technology involving indirect liquefaction of coal to transportation fuels (Kolbel and Ralek, 1980). This process involves the use of synthesis gas with a relatively low hydrogen to carbon monoxide ratio (0.6-0.7), which is bubbled through a slurry of finely divided catalyst, suspended in a heavy oil medium, whose composition may or may not change with time, depending upon the product selectivity variation with time.

One of the major advantages in using a bubble column slurry reactor (BCSR) is its excellent temperature uniformity and control. This is due to the thorough mixing of the slurry, which also possesses a high heat capacity and hence, efficient heat transfer capability. The formation of local hot-spots is therefore prevented thereby reducing the destruction of catalyst and production of methane. The conversion of gaseous reactants to the desired

products is high for a single pass, and catalyst ageing is not a problem because carbon deposition is greatly suppressed. Furthermore, since the design of such a reactor is simple, its capital cost per unit reactor volume is also low.

Many experimental attempts on the use of BCSR for the F-T synthesis have been reported. (Schlesinger, et al., 1954), (Mitra and Roy, 1963), (Farley and Ray, 1964), (Sakai and Kunugi, 1974). The first successful operation of a large-scale demonstration plant was started in 1953, at Rheinpreussen-Koppers, as described by Kolbel and Ralek (1980). The slurry reactor consisted of a pressure-resistant steel vessel of diameter 1.55m and a height of 8.6m (Figure I-B-1). The results obtained during the operation of the demonstration plant, along with the economically important consumption data, formed the basis of the offer made by Heinrich Kopper GmBH, to the Indian Government to build a complete liquid-phase synthesis plant, but due to a switch from coal to petroleum feed stock, these plans were shelved.

With the view of a proper design, scale-up, simulation, control and optimization of the indirect coal liquefaction process employing F-T synthesis, in a BCSR, an appropriate model, based on mechanistic details, is essential. A F-T slurry reactor is a complicated system whose adequate understanding requires resolution of problems involving F-T chemistry, reaction kinetics, hydrodynamics and transport processes in relation to mass, momentum and energy. In the general case of the F-T slurry reactor, the following specific transport and kinetic processes are commonly encountered: (Figure I-B-2).

1. Transfer of the reactants from the bulk gas phase to the gas-liquid interface.

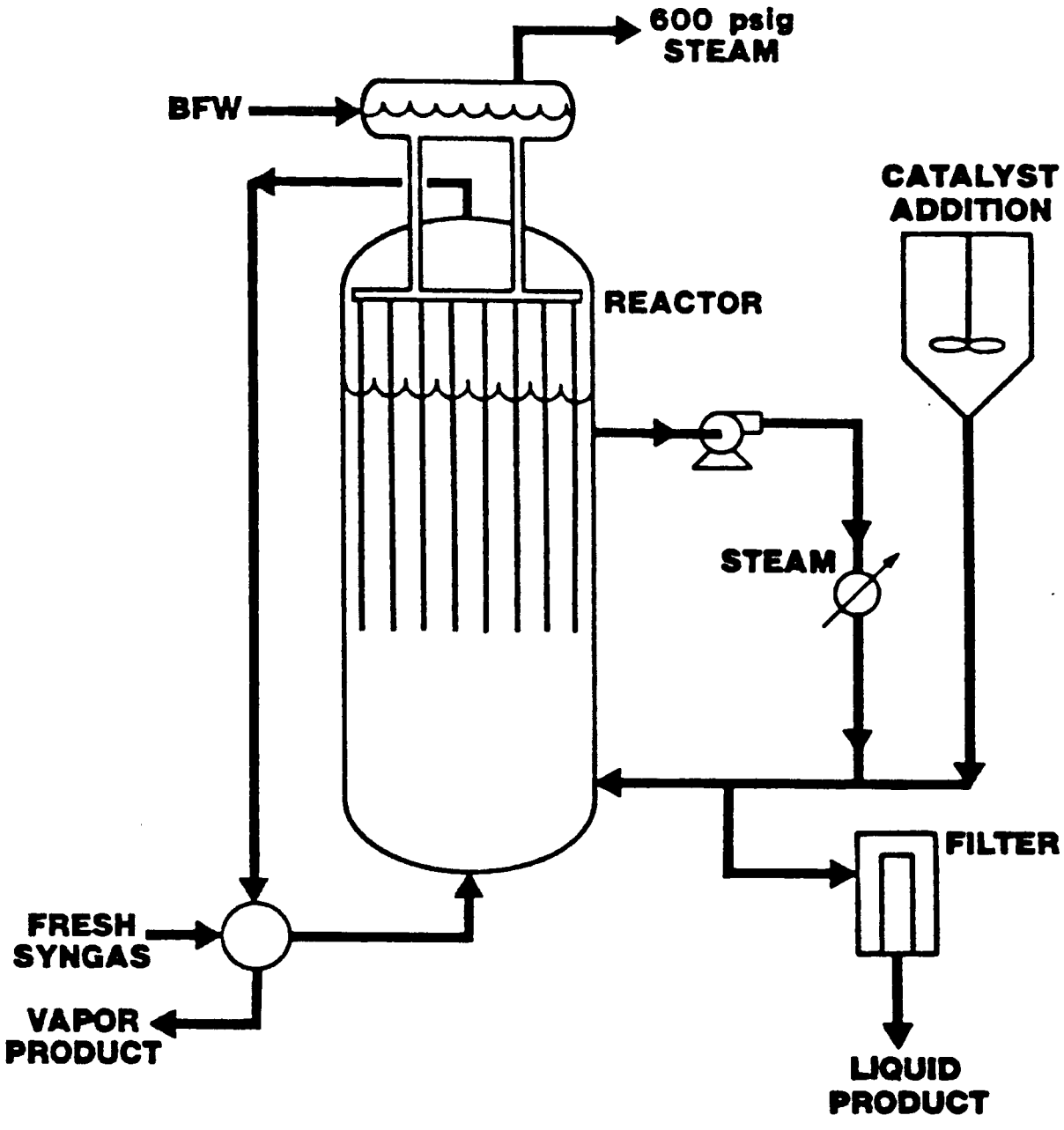

Figure I-B-1: Bubble Column Slurry Reactor (BCSR)

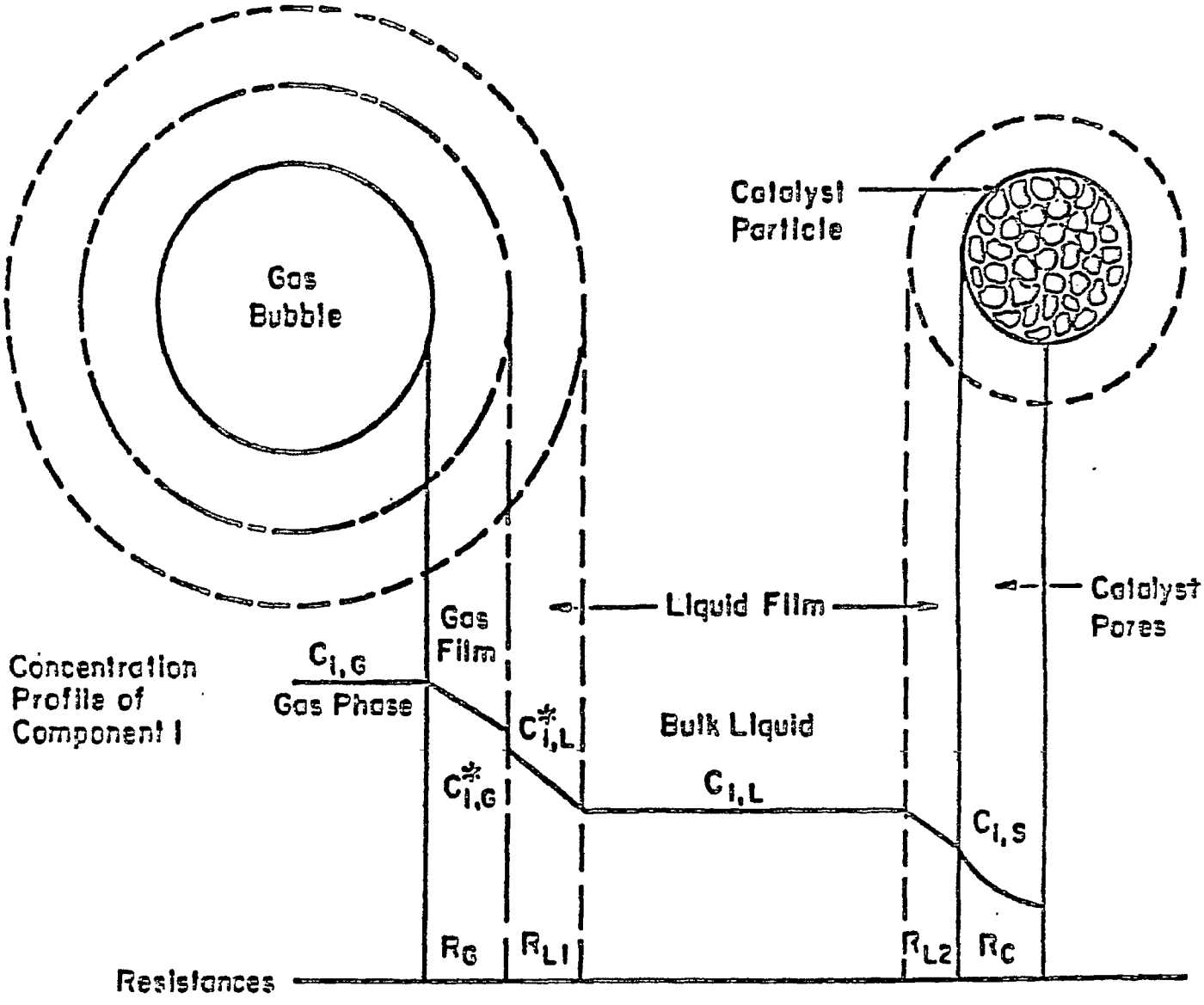

Figure I-B-2: Transport and Kinetic Processes involved in BCSR

2. Transfer of the reactants from the gas-liquid interface to the bulk liquid phase.

3. Mixing and diffusion of the reactants in the bulk liquid phase.

4. Transfer of the reactants to the external surface of the catalyst particles.

5. Diffusion of the reactants to the catalyst interior.

6. Conversion of the reactants inside the catalyst pores.

7. Diffusion of reaction products from the active sites to the catalyst particle surface.

8. Transfer of the products from the catalyst to the bulk liquid phase.

9. Transfer of the products from the bulk liquid to the gas liquid interface.

10. Transfer of the products from the gas-liquid interface to the bulk gas.

Out of all the above steps, the largest resistance is the one offered by the surface reaction. However, resistance attributed to the diffusion of reactants, viz., H_2 and CO from the gas-liquid interface to the bulk liquid is also important, while the other resistances may be ignored.

Specific models for F-T slurry reactors have been developed by considering these process details under steady state conditions. Besides considering the above steps, one has to also account for the flow patterns for the gas phase, the slurry phase, and the solid catalyst. These flow patterns define the concentration profiles in the reactor and therefore influence the syngas conversions. Mathematical models for the F-T synthesis in slurry reactors have been developed by six different groups of workers. (Deckwer et al., 1982; Calderbank et al., 1963; Satterfield and Huff, 1980; Bukur, 1983;

Kuo et al., 1983; Stern et al., 1985a). A detailed review of these models along with their relative merits and demerits has been given by Saxena et al. (1985).

In the present work, two different models, which are somewhat parallel to those reported earlier, have been developed to describe the performance of BCSR with F-T synthesis.

BCSR Model 1

The description of F-T synthesis in the slurry phase essentially represents the modeling of a three-phase reactor system. In order to estimate the behavior and performance of large-scale F-T slurry reactors, characterized by a large length to diameter ratio, the design equations should necessarily be based on the dispersion model (Mhashkar, 1974); (Deckwer, 1976).

a. Model Assumptions: The model equations used to simulate the performance of BCSR are based on the following assumptions,

i) Steady state operation

ii) No temperature variation along the reactor i.e. isothermal condition

iii) Since the total pressure is comparatively greater than the pressure drop, the reactor is assumed to operate under iosbaric conditions.

iv) The gas phase is assumed to behave ideally.

v) The reactor operation is semibatch with continuous bubbling of gas.

vi) Radial gradients of concentration are absent.

vii) The reaction kinetics is first order with respect to hydrogen concentration, i.e., $\gamma_{H2} = K_H C_{LH}$, typical of F-T

synthesis over Fe catalyst for a CO rich synthesis gas (Dry et al., 1976).

viii) Axial dispersion is considered in both the gas as well as the liquid phase.

ix) Catalyst particle size is sufficiently small to neglect pore diffusion, but large enough for mass transfer and chemical reaction to be in series.

b. Model Equations: The following dimensionless variables have been used while developing the model equations:

$$\Theta_{GH} = \frac{C_{GH}}{C_{GHO}}, \quad \Theta_{LH} = \frac{C_{LH}\, m_H}{C_{GHO}}, \quad \Theta_G = \frac{C_G}{C_{GHO}}$$

$$\bar{U}_G = \frac{U_G}{U_G^{\,o}}, \quad z = \frac{x}{L} \qquad (1)$$

The dimensionless groups appearing in the model equations are:

$$Pe_{GH} = \frac{U_G^{\,o} L}{D_{GH}}, \quad St_{GH} = \frac{K_{LH}\, a\, L}{m_H\, U_G^{\,o}} \qquad (2)$$

$$Pe_{LH} = \frac{U_G^{\,o} L}{D_{LH}}$$

The gas phase mass balance for hydrogen is then given by:

$$\frac{1}{(Pe)_{GH}} \frac{d}{dz}\left[\varepsilon_G \frac{d\,\Theta_{GH}}{dz}\right] - \frac{d}{dz}\left[\bar{U}_G\, \Theta_{GH}\right] - (St)_{GH}\left[\Theta_{GH} - \Theta_{LH}\right] = 0 \qquad (3)$$

with the boundary conditions:

$$\bar{U}_G \Theta_{GH} - \frac{\varepsilon_G}{(Pe)_{GH}} \left(\frac{d\Theta_{GH}}{dz}\right) = 1 \qquad @\ z = 0 \tag{4}$$

$$\frac{d\Theta_{GH}}{dz} = 0 \qquad @\ z = 1 \tag{5}$$

The mass balance for H_2 in the liquid phase is:

$$K_{LH}\underline{a}\ (C_{GH}^{*} - C_{LH}) + D_{LH}\frac{d}{dx}\left[\varepsilon_L \frac{dC_{LH}}{dx}\right] - \left[K_{SL}\ \underline{a}_{SL}\ (C_{LH} - C_{SH})\right] = 0 \tag{6}$$

The component transferred across the solid-liquid interface reacts at the catalyst surface for which,

$$K_{SL}\ \underline{a}_{SL}\ (C_{LH} - C_{SH}) = \gamma_{H_2} = K_H \varepsilon_L C_{cat} C_{SH} \tag{7}$$

However, taking into consideration a finite resistance at the solid-liquid interface, as given by:

$$\eta = \frac{1}{1 + \dfrac{K_H C_{cat} \varepsilon_L}{K_{SL}\underline{a}_{SL}}} \tag{8}$$

The surface concentration of H_2 can be related to the bulk liquid phase concentration by,

$$C_{H,S} = \eta\ C_{HL} \tag{9}$$

Hence, the liquid phase component balance, expressed in dimensionless form is given by:

$$(St)_{CH}\, m_H\, (\Theta_{GH}-\Theta_{LH}) + \frac{1}{(Pe)_{LH}} \frac{d}{dz} \left[\varepsilon_L \frac{d\Theta_{LH}}{dz}\right] - \left[\frac{C_{cat} K \varepsilon_L Ln}{U_{Go}}\right] \Theta_{LH} = 0 \qquad (10)$$

with the boundary conditions:

$$\frac{d\Theta_{LH}}{dz} = 0 \qquad @\ z = 0 \qquad (11)$$

$$\frac{d\Theta_{LH}}{dz} = 0 \qquad @\ z = 1 \qquad (12)$$

The variation of the superficial gas velocity along the reactor height, is accounted for, by applying the concept of contraction factor α, as defined by Levenspiel (1972)

$$U_G = U_G^{o}\, (1 + \alpha\, X_{CO + H_2})$$

$$\text{where, } \alpha = \frac{(U_G)_{x=1} - (U_G)_{x=0}}{(U_G)_{x=0}} \qquad (13)$$

The value of α for a F-T slurry reactor varies between -0.5 and -0.6 (Deckwer et al., 1981). Although this assumption may not be generally valid over the the entire range of conversions its use greatly simplifies the analysis.

The rate of synthesis gas consumption is related to the rate of consumption of H_2 by,

$$\gamma_{CO + H_2} = (1+U)\ \gamma_{H_2}$$

where U, is the ratio of moles of CO consumed to the moles of H_2 consumed. With a view of overcoming the problem associated with the varying stoichiometry of F-T synthesis, the usage ratio is set equal to the inlet molar ratio of CO to H_2.

The syngas conversion is thus related to the hydrogen conversion by the relation,

$$X_{CO + H_2} = \left(\frac{1+U}{1+I}\right) X_{H_2} \qquad (14)$$

where,

$$X_{H_2} = \frac{U_G^{\circ}\ C_{GHO} - U_G\ C_{GH}}{U_G^{\circ}\ C_{GHO}} = 1 - \bar{U}_G \Theta_{GH} \qquad (15)$$

Defining,

$$\alpha^* = \alpha\ \left(\frac{1+U}{1+I}\right) \qquad (16)$$

one can express,

$$\frac{U_G}{U_G^{\circ}} = \bar{U}_G = \frac{1 + \alpha^*}{1+\alpha^*\ \Theta_{GH}} \qquad (17)$$

and the variation of superficial gas velocity along the reactor height, is given by,

$$\frac{d\bar{U}_G}{dz} = \frac{(1+\alpha^*)\ \alpha^*}{(1+\alpha^*\ \Theta_{GH})^2}\ \frac{d\Theta_{GH}}{dz} \qquad (18)$$

With the view of establishing, the catalyst concentration profile along the reactor, use is made of the sedimentation dispersion model as applied for a semibatch operation,

$$E_s \frac{d^2C_{cat}}{dx^2} + U_{cs} \frac{dC_{cat}}{dx} = 0 \qquad (19)$$

with the boundary conditions,

$$\frac{dC_{cat}}{dx} = 0 \qquad \begin{matrix} @\ x = 0 \\ @\ x = L \end{matrix} \qquad (20)$$

The physico-chemical properties of the liquid, the slurry, and the gas, along with the various hydrodynamic parameters pertinent to the BCSR operation, have been estimated from correlations reported in literature. Each of these correlations is built into the simulator in the form of subroutines, which can be called as when required. This facilitates an easy updating by the user. The correlations used are given in Table I-B-1.

c. Numerical Solution: Equations (3) and (10), along with the boundary conditions, constitute a boundary value problem. These equations were solved numerically, using the algorithm, COLSYS (Ascher et al., 1981). The algorithm uses the method of spline collocation at Gaussian points. Equation (19) was solved analytically, to establish the catalyst concentration profile along the reactor.

Table I-B-1

Correlations for the Estimation of Physico-Chemical and Hydrodynamic Properties Used in BCSR Model 1

1. Liquid Density:

(Deckwer, 1980)

$$\rho_L = 0.758 - 0.555 \times 10^{-3} (T-273) \quad gm/cm^3$$

2. Liquid Viscosity:

(Deckwer, 1980)

$$\mu_L = 0.052 \exp (-6.905 + 3266/T) \quad gm/cm/sec$$

3. Volume Fraction of Solids:

$$V_{cat} = \frac{\rho_L W_{cat}}{\rho_{cat} - W_{cat} (\rho_{cat} - \rho_L)}$$

where

$$W_{cat} = \text{catalyst loading} = \frac{m_{cat}}{m_{sus}}$$

4. Slurry Density:

$$\rho_{SL} = V_{cat} \rho_{cat} + (1-V_{cat}) \rho_L \quad gm/cm^3$$

5. Slurry Viscosity:

$$\mu_{SL} = \mu_L (1 + 4.5 V_{cat}) \quad gm/cm/sec$$

6. Gas Holdup:

(Deckwer, 1980)

$$\varepsilon_G = 0.053 U_G^{1.1}$$

7. Gas-Liquid Interfacial Area:

(Deckwer, 1980)

$$\underline{a} = 4.5 U_G^{1.1} \quad cm^{-1}$$

8. Gas-Liquid Mass Transfer Coefficient:

(Satterfield and Huff, 1980)

$$K_{LH} = 0.1165 \left(\frac{\rho_{SL}}{\mu_{SL}} \exp \left(-\frac{4570}{T}\right)\right)^{1/3} \quad cm/sec$$

9. Solid-Liquid Interfacial Area:

(Sanger and Deckwer, 1981)

$$a_s = 6\left[\frac{W_{cat}\,(1-\varepsilon_G)\,\rho_{SL}}{d_{cat}\,\rho_{cat}}\right]$$

10. Solid-Liquid Mass Transfer Coefficient:

(Sanger and Deckwer, 1981)

$$K_s = \frac{D_L}{d_{cat}}\left(2 + 0.545\left(\frac{\mu_L}{\rho_L D_L}\right)^{1/3}\left(\frac{\varepsilon\, d_{cat}^{\,4}\,\rho_L^{\,3}}{\mu_L^{\,3}}\right)\right)$$

where, $\varepsilon = U_G g$ for $U_G \leq 6$ cm/sec

$\varepsilon = 5886\ cm^2/sec^3$ for $U_G > 6$ cm/sec

11. Gas Phase Dispersion Coefficient:

(Mangartz and Pilhofer, 1980) (Deckwer, 1982)

$$D_G = 5\times10^{-4}\left(\frac{U_G}{\varepsilon_G}\right) d_R^{\,1.5}\ cm^2/sec$$

12. Liquid Phase Dispersion Coefficient:

(Shah and Deckwer, 1981)

$$D_L = 3.67\,(U_G)^{0.32}\,(d_R)^{1.34}\ cm^2/sec$$

13. Solids Distribution:

$$C_{cat} = C_s^{\,o}\exp\left[-\frac{\psi_L U_{cs} Lx}{Es}\right]$$

where

$$C_s^{\,o} = \frac{\overline{C}_s\, A}{\exp[A] - 1}$$

$$A = -\frac{\psi_L U_p L}{Es}$$

$$Es = \frac{U_G\, d_R\,(1 + 8\,Fr^{0.85})}{13\,Fr}$$

$$Fr = \frac{U_G}{\sqrt{g\, d_R}}$$

$$U_{cs} = 1.2\,U_{ct}\left(\frac{U_G}{U_{ct}}\right)^{0.25}\left(\frac{1 - V_{cat}}{1 - V_{cat}^{*}}\right)^{2.5}$$

where, V^*_{cat} is the volume fraction of catalyst for C_{cat} = 0.1 gm/cc

The terminal setting velocity is given by

$$Re = \frac{U_{ct}\ d_{cat}\ \rho_L}{\mu_L}$$

where, $Re = \frac{Ar}{18}$ for $Re \leq 0.5$

$$Re = \left(\frac{Ar}{13.9}\right)^{0.7} \quad \text{for } Re > 0.5$$

and $$Ar = \frac{\rho_L\ (\rho_{cat} - \rho_L)\ g\ d^3_{cat}}{\mu_L^2}$$

14. Kinetic Parameters:

(Deckwer et al., 1980)

$$K_H = \frac{K'_{fo}}{1+U} \exp\left(-\frac{E_a}{RT}\right)$$

where, $K'_{fo} = 1.12 \times 10^5$ (sec % Fe)$^{-1}$

E_a = 70 kJ/mol

d. Parameter Effect on Reactor Performance

A parametric study was performed to test the simulator, by varying the operating and design conditions. The trends obtained in the values of syngas conversion are satisfactory and can be explained based on theoretical and experimental observations. Following is a brief discussion about the effect of various operating and design parameters on the reactor performance.

. Effect of Pressure

The operating pressure has no effect on the conversion of synthesis gas along the reactor, as can be seen from the flat profile as shown in Figure I-B-3. However, this effect is observed, since the reactor is assumed to be operated under isothermal conditions, but under non-isothermal conditions, the conversion would increase with increasing pressure. Variation of the space time yield (STY) with pressure illustrated in Fig. I-B-4 shows a linear profile which is mainly the result of the first order kinetic expression used in the model equations.

Effect of Inlet Gas Velocity

An increase in the inlet gas velocity leads to a drop in the syn-gas conversion, as shown in Figure I-B-5. This may be attributed to a decrease in the residence time of the reactants and an increased liquid phase dispersion, for a particular set of design parameters. However, the STY goes through a maximum with an increase in velocity as shown in Fig. I-B-6. The optimum inlet gas velocity obtained lies in the range of velocity used in the Rheinpreussen-Koppers plant. Such a maximum is obtained since F-T synthesis in the slurry phase takes place in an absorption-with-slow-reaction regime. (Satterfield and Huff, 1980). Thus if the reactor does not operate under

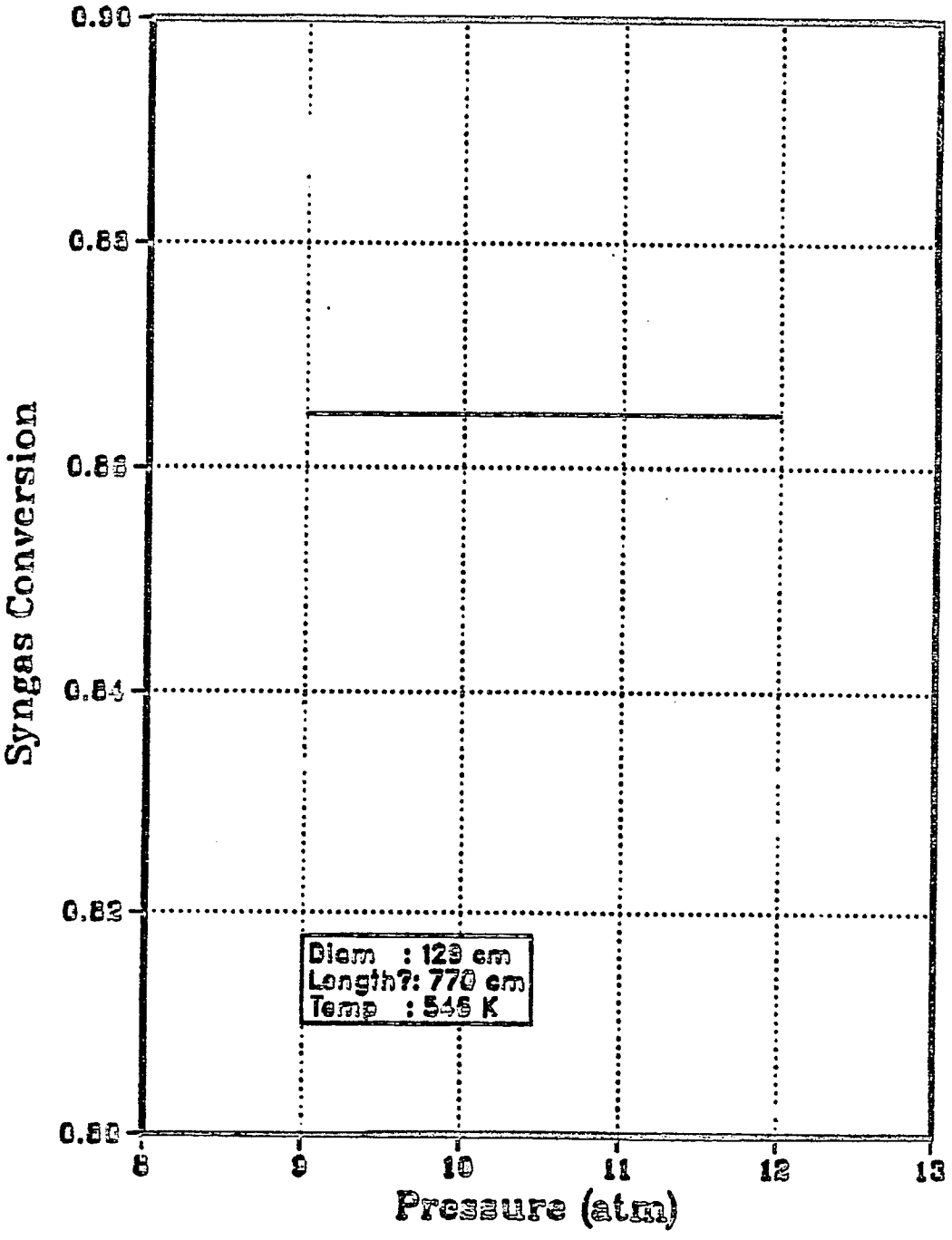

Figure I-B-3: Effe t of Pressure on Syngas Conversion

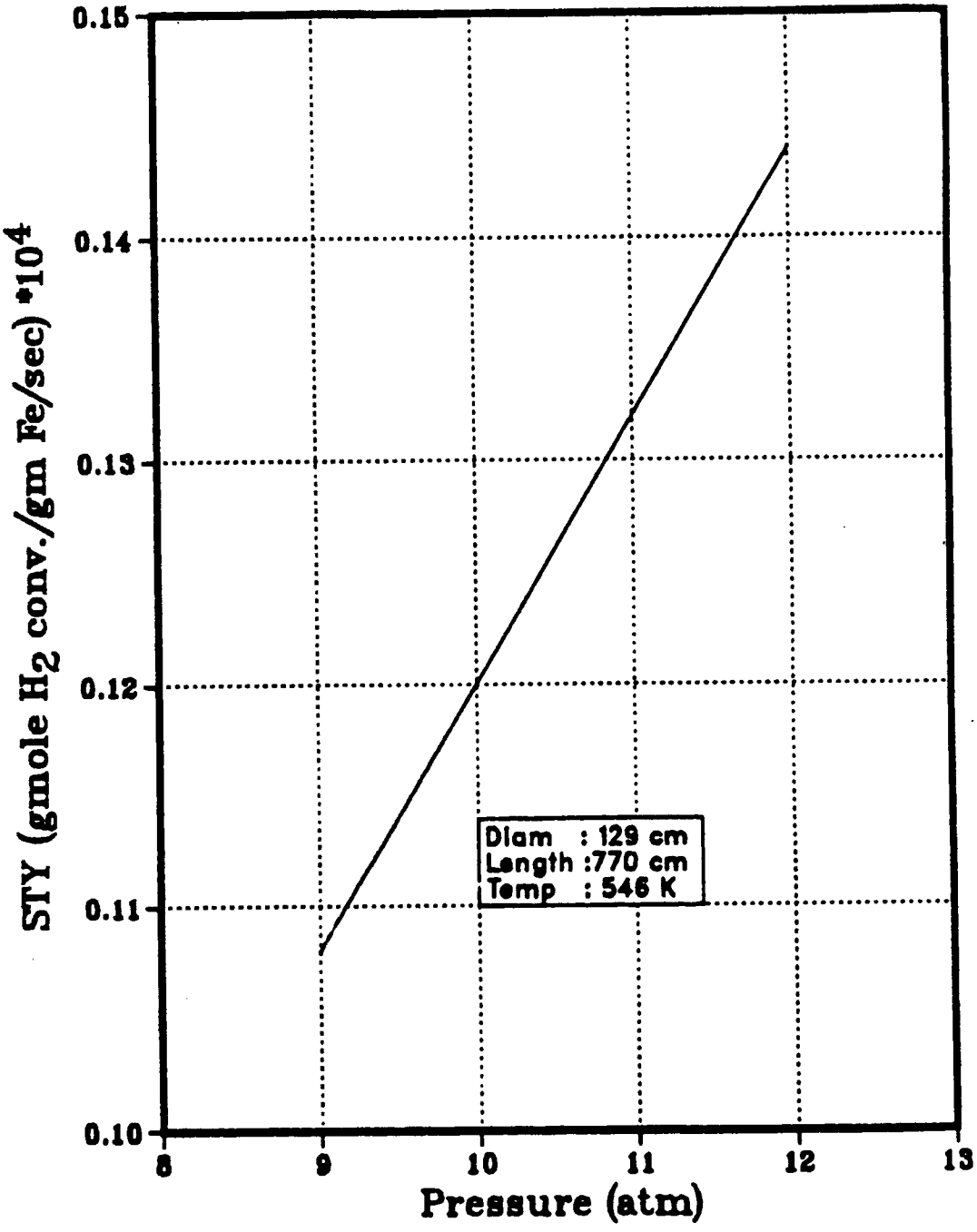

Figure I-B-4: Effect of Pressure on STY

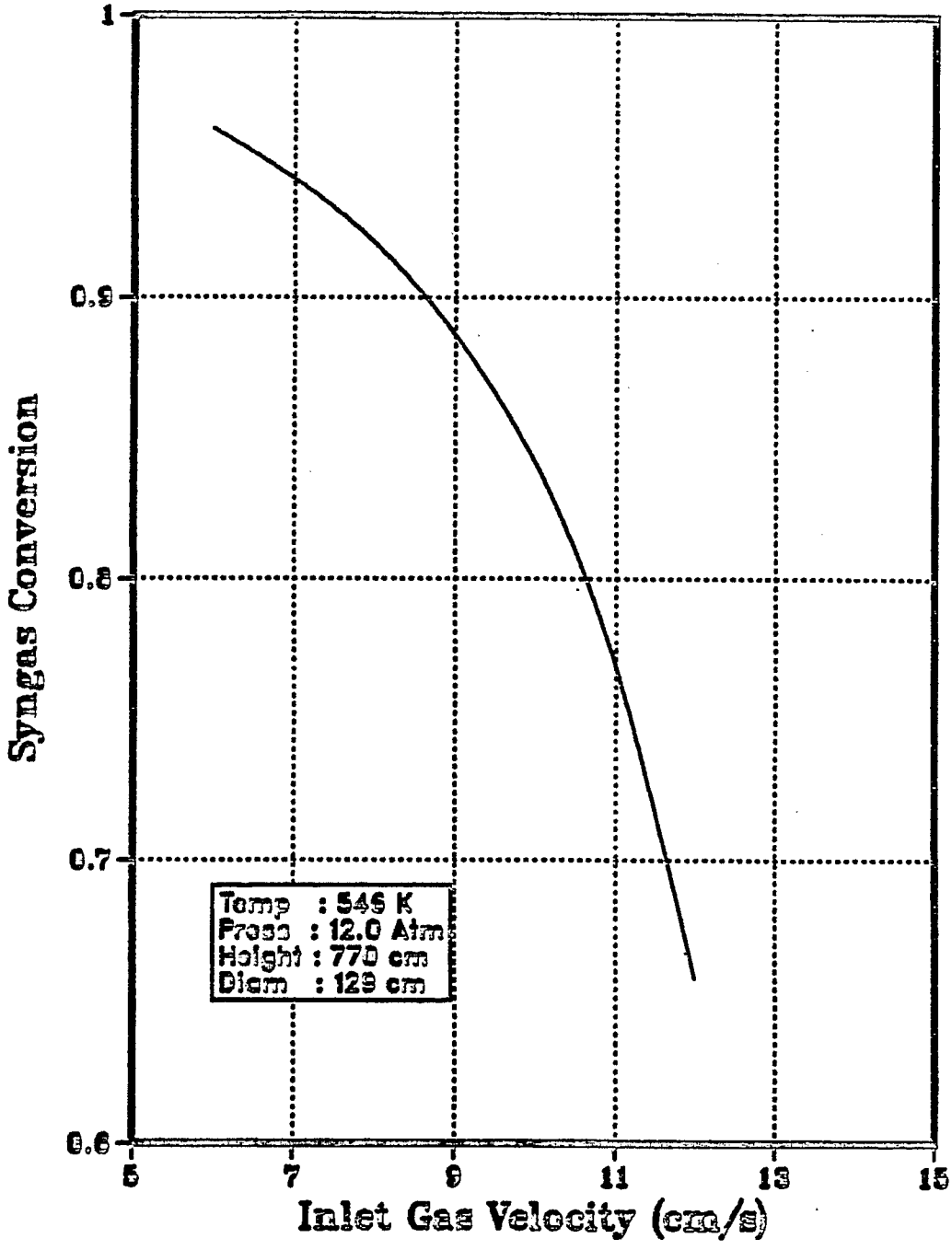

Figure I-B-5: Effect of Inlet Gas Velocity on Syngas Conversion

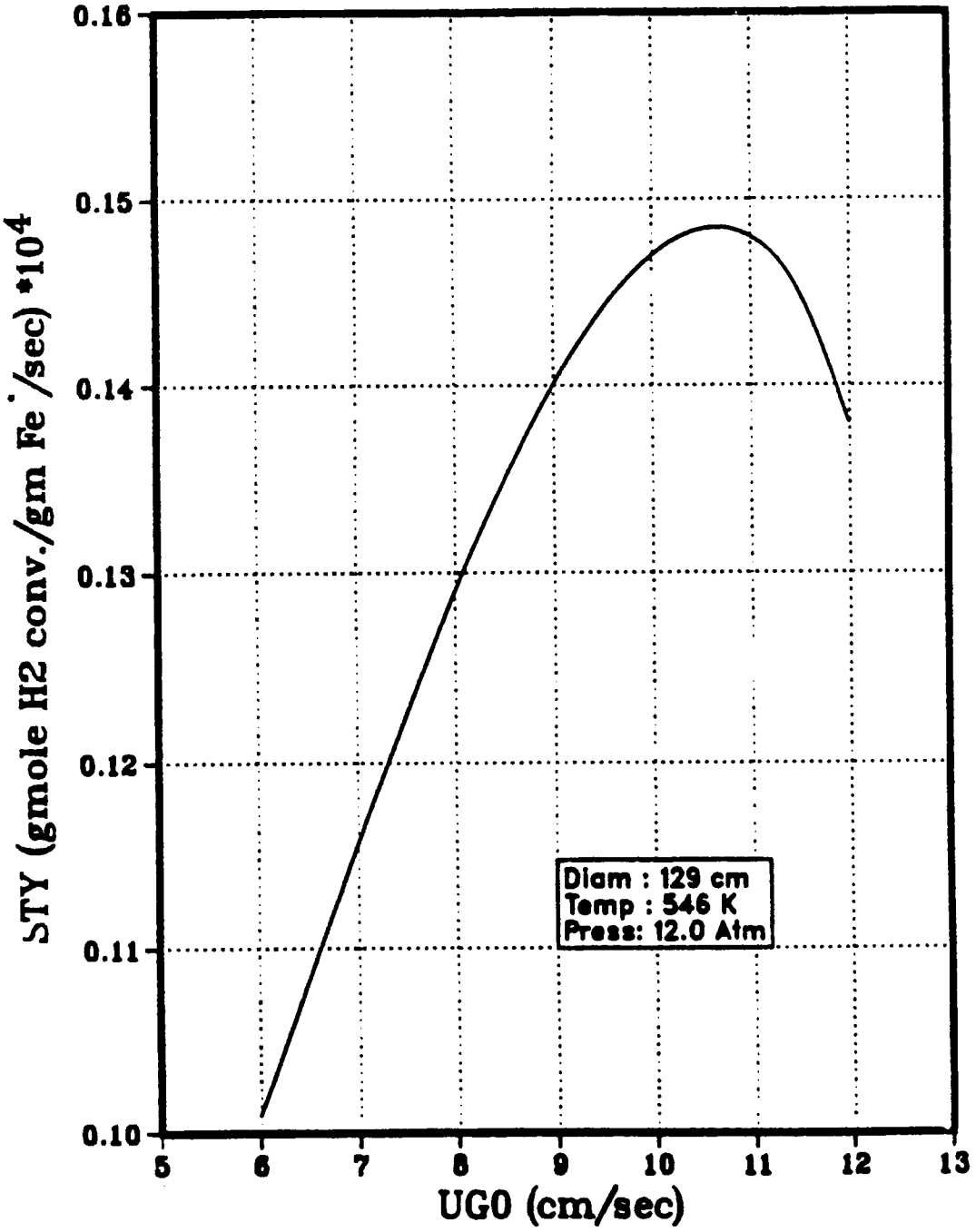

Figure I-B-6: Effect of Inlet Gas Velocity on ST

optimum conditions with regard to high space-time yield, the relative kinetic resitance may be smaller and hence the overall process may be more and more mass transfer controlled.

- Effect of Reactor Diameter

Although the effect of increasing the reactor diameter on syn-gas conversion is not pronounced, as shown in Figure I-B-7, one does observe a drop in conversion, with an increase in the reactor diameter, which may be attributed to the increase in the level of axial dispersion due to increased backmixing.

- Effect of Reactor Length

Increase in the length of the reactor leads to an obvious increase in the syn-gas conversion, due to an increase in the reactor volume and hence, the reactant residence time, for a constant inlet superficial gas velocity. The variation of syn-gas conversion with the reactor height is shown in Figure I-B-8. The figure also illustrates the effect of reactor diameter on the level of conversion, which drops with an increase in the reactor diameter.

BCSR Model 2

F-T reaction may be defined as the catalytic polymerization and hydrogenation of CO to give hydrocarbons and oxygenated products with various chain lengths, along with H_2O and CO_2. The literature contains a plethora of product selectivities obtained from various catalysts (mostly Fe, Co, Ru and Ni) under a variety of reaction conditions. A study of all the data, that has been collected to date, has revealed that there is a definite inter-relationship among the various products (Dry, 1981). Thus, if selectivity of

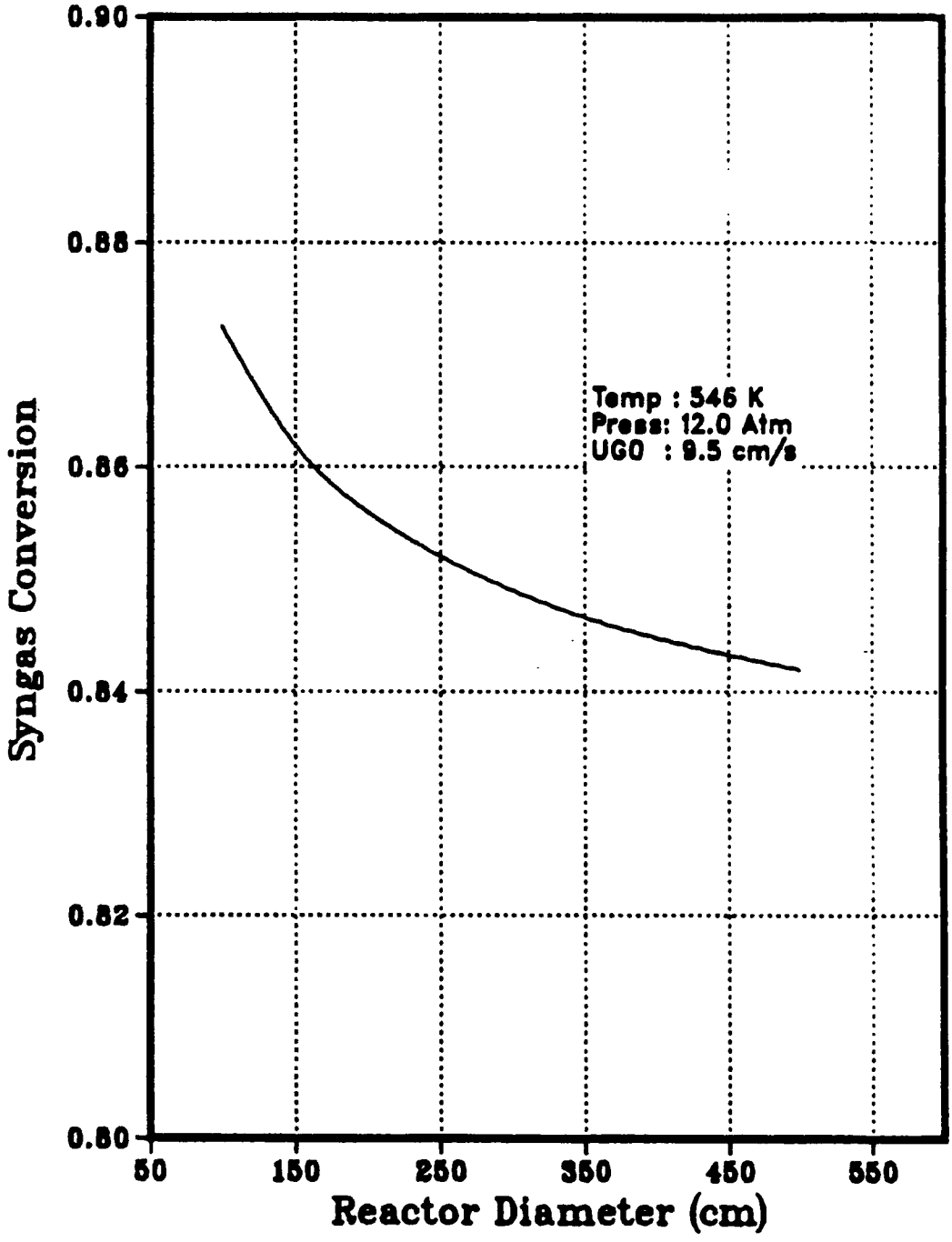

Figure I-B-7: Effect of Reactor Diameter on Syngas Conversion

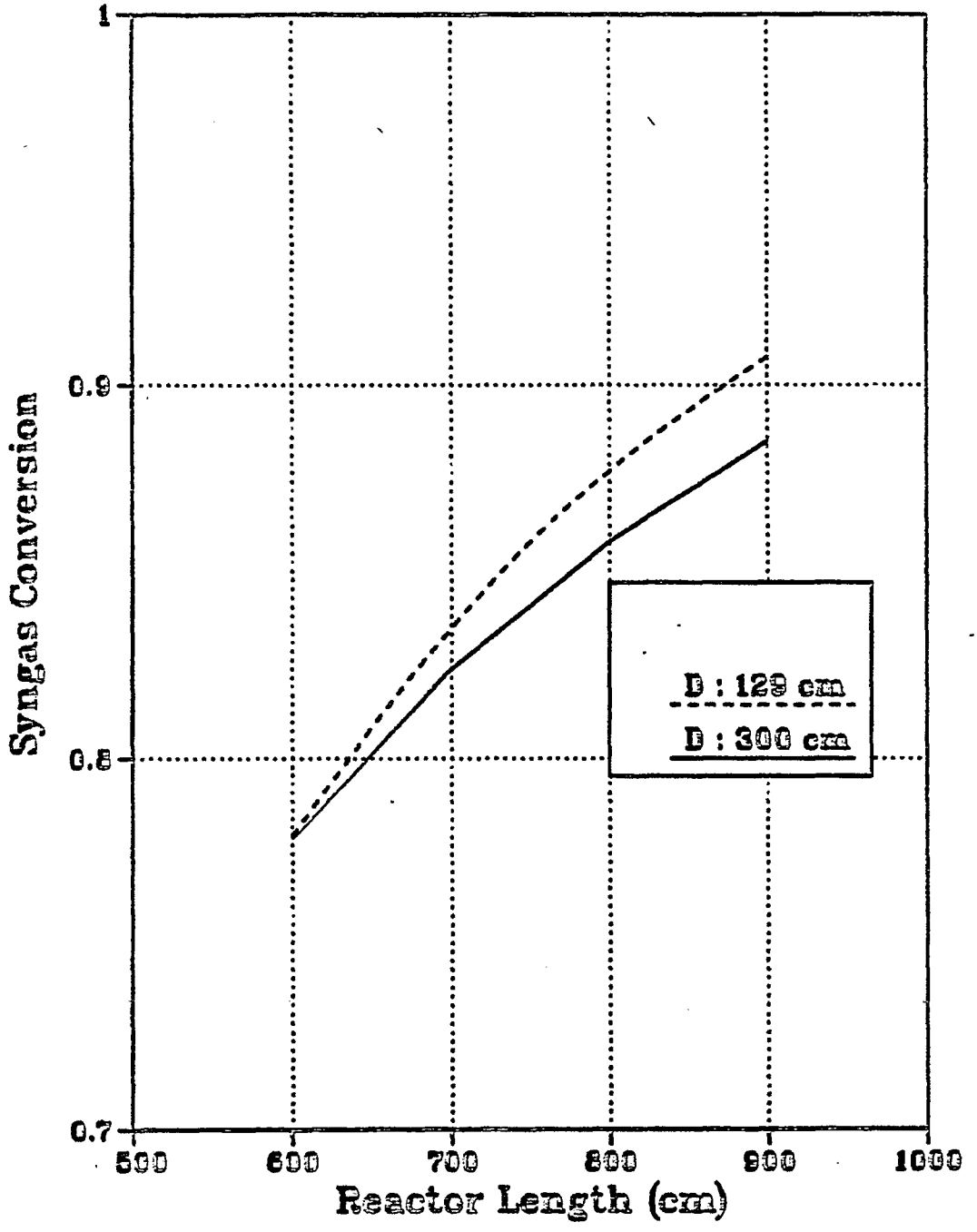

Figure I-B-8: Effect of Reactor Length on Syngas Conversion

a particular carbon number species is changed, then the selectivities of all the other carbon number species will also change by a predictable amount, irrespective of the source of this change, whether by a change in the catalyst used or by a change in the F-T process conditions.

The product distribution obtained in a typical F-T synthesis operation can be closely approximated using a Schulz-Flory distribution. The reaction mechanism involves the steps of chain initiation, chain propagation and chain termination. Carbon chain growth occurs by the addition of one carbon at a time, while termination leads to prompt desorption of the molecule from the catalyst site. The probability that a hydrocarbon chain will grow rather than terminate, is given by a chain growth probability factor, α, which is defined as,

$$\alpha = \frac{K_g}{K_g + K_t}$$

where, K_g = rate constant for chain growth

K_t = rate constant for chain termination

Thus, in the limit, $\alpha = 1$, indicates growth without termination, while $\alpha = 0$, indicates chain termination. The chain growth probability factor is characteristic of the catalyst system and the operating conditions. It has been observed that α does not vary strongly with the H_2/CO ratio, but decreases with an increase in the reaction temperature, as shown in Figure I-B-9 (Stern et al., 1985b). Furthermore, experimental evidence with F-T catalysts has shown that high molecular weight products (C_5+) fall on a straight line, typical of a Schulz-Flory distribution, the intercept with the ordinate being less than unity, with the low molecular weight products falling

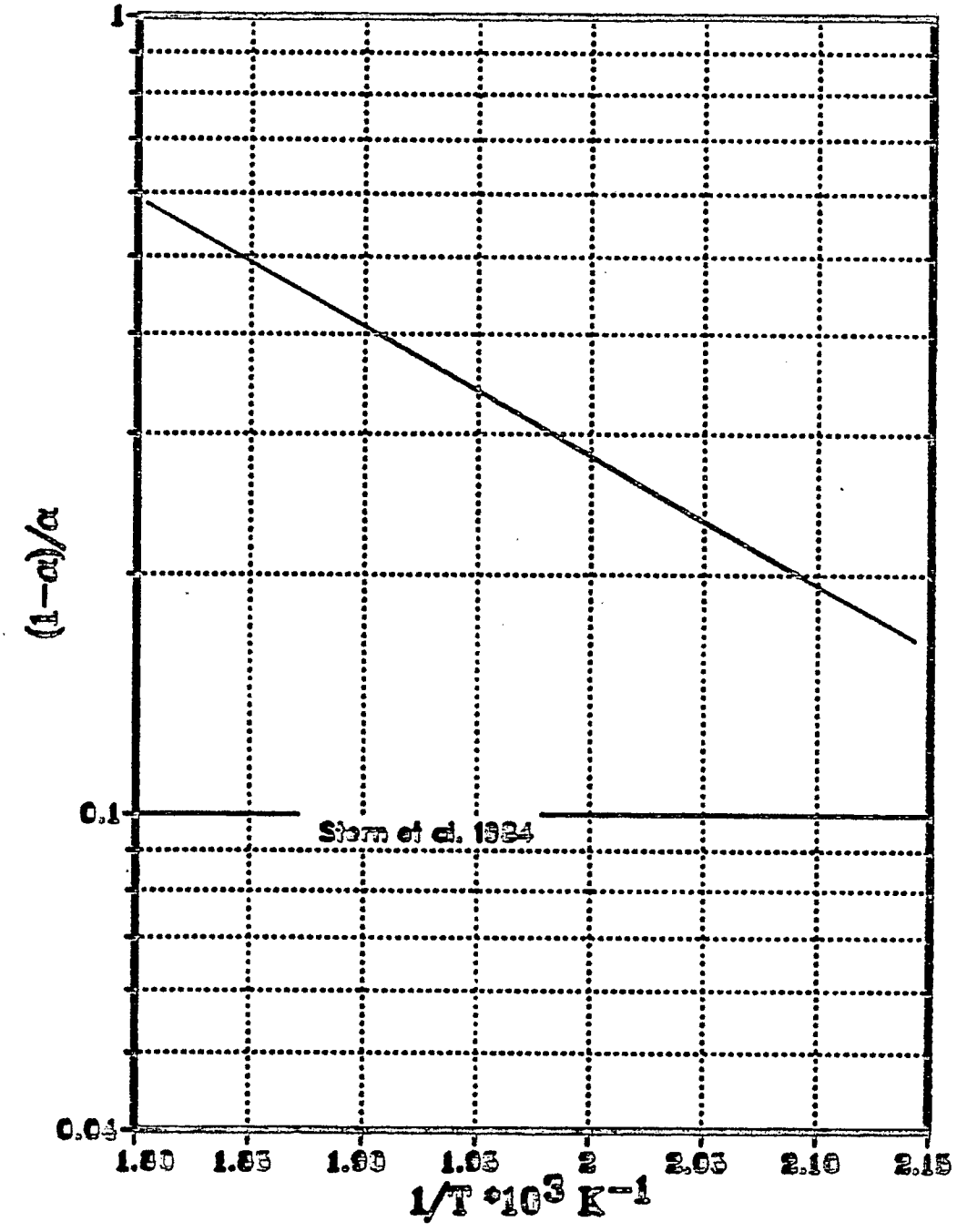

Figure I-B-9: Variation of Chain Growth Probability Factor with Temperature

below the straight line. This indicates that the relative rates of chain propogation and termination depend on the length of the chain for short chain lengths ($n \leq 5$).

Based on the above observations and the experimental data obtained for F-T synthesis over a Ru/Al_2O_3 catalyst, the rates of formation of C_1-C_4 products are described by a power law kinetic expression (Stern et al., 1985b)

$$\gamma_{C_n} = A_n \exp\left(\frac{-E_n}{RT}\right) P_{H_2}^{a_n} P_{CO}^{b_n} \qquad \text{for } n = 1,2,3,4$$

Since, the value of α does not depend on the carbon number of products containing roughly more than four carbon atoms, the rates of formation of higher products can be determined using the expression,

$$\gamma_{C_n} = \alpha^{n-4} \gamma_{C_4} \qquad \text{for } n \geq 5$$

The study of F-T synthesis over Ru catalysts began in 1930, when Pichler obtained very high molecular weight waxes. Ruthenium catalysts are active over a wide range of operating conditions: temperatures from 100 to 300°C and pressures from 1 to 2000 atm, with selectivity varying from the production of all CH_4 to "polymethylene". Water is usually the principal oxygen-containing product. (Anderson, 1984) The activity of Ru at low temperature is higher than that of common F-T catalysts, Ni, Co, and Fe. It is a versatile catalyst, in that at higher temperatures it is an excellent methanation catalyst while at low temperatures and high pressures it produces large amounts of very high molecular mass waxes. It is most active in the pure metal form; i.e. supports and/or promoters appear to have no beneficial effect. Even under conditions of high wax yields, Ru tends to have a high CH_4

selectivity. The waxes are oxygen free and highly paraffinic. (Dry, 1981)

a. Model Assumptions

The mathematical model developed to predict the product distribution of a F-T bubble column reactor is based on the following assumptions:

i) Steady state operation

ii) No temperature variation along the reactor, i.e. isothermal condition.

iii) Reactor is assumed to operate at constant pressure.

iv) The reactor is operated in a semibatch manner.

v) Radial gradients in concentration are negligible.

vi) Gas phase is assumed to obey ideal gas law.

vii) Equations assuming plug flow in the gas and the liquid phase and a more general axial dispersion flow have been developed.

viii) The kinetic parameters used are those reported for F-T synthesis over Ru/Al_2O_3 catalysts (Stern et al., 1985b).

b. Model Equations

The model equations are expressed in terms of the following dimensionless variables:

$$\theta_{G_i} = \frac{C_{G_i}}{C_{GHo}}, \qquad \theta_{L_i} = \frac{C_{L_i} m_i}{C_{GHo}}, \quad z = \frac{x}{L} \tag{21}$$

$$\theta_G = \frac{C_G}{C_{GHo}}, \qquad \overline{U}_G = \frac{U_G}{U_G^o}$$

(i) Plug flow assumption in gas and liquid phase:

The component balance in the gas phase is given by

$$\frac{-d(\overline{U}_G \theta_{G_i})}{dz} - N_i(\theta_{G_i} - \theta_{L_i}) = 0 \tag{22}$$

where, N_i = Stanton number = $\dfrac{K_{L_i} \frac{a}{} L}{m_i U_G^o}$

The boundary condition to be satisfied is,

$$\theta_{G_i} = \theta_{G_i}^o \qquad @\ z = 0 \qquad (23)$$

The liquid phase component balance is given by,

$$N_i(\theta_{G_i} - \theta_{L_i}) + \rho_i = 0 \qquad (24)$$

where, ρ_i accounts for the net formation of a species due to kinetic reaction, i.e., ρ_i is -ve for the reactants and +ve for the products.

Assuming the following reaction stoichiometry,

$$(2n+1)H_2 + nCO \xrightarrow[cat]{} C_nH_{2n+2} + nH_2O$$

the expressions for ρ_i for the various components can be expressed as,

$$\rho_{H_2} = -\sum_{n=1}^{3}(2n+1)Da_{c_n}\theta_{LH}^{an}\theta_{L_{CO}}^{bn} - Da_{c_4}\theta_{LH}^{a_4}\theta_{L_{CO}}^{b_4}\sum_{n=4}^{\infty}(2n+1)\alpha^{n-4} \qquad (25)$$

$$\rho_{CO} = -\sum_{n=1}^{3} nDa_{c_n}\theta_{L_H}^{an}\theta_{L_{CO}}^{bn} - Da_{c_4}\theta_{L_H}^{a_4}\theta_{L_{CO}}^{b_4}\sum_{n=4}^{\infty} n\alpha^{n-4} \qquad (26)$$

$$\rho_{c_n} = Da_{c_n}\theta_{LH}^{an}\theta_{L_{CO}}^{bn} \qquad \text{for } n = 1,2,3 \qquad (27)$$

$$\rho_{c_n} = Da_{c_n}\theta_{LH}^{a_4}\theta_{L_{CO}}^{b_4}\alpha^{n-4} \qquad \text{for } n = 4,5,\ldots\infty \qquad (28)$$

$$\rho_{H_2O} = -\rho_{CO} \qquad (29)$$

where, Da_{c_n} represents the Damkohler number for hydrocarbons containing one to four carbon numbers:

$$Da_{cn} = \frac{C_{cat} L(1-\varepsilon_G) B_n (C_{GHO})^{an+bn-1} (RT)^{an+bn}}{U_G^o \, m_H^{an} \, m_{CO}^{bn}} \qquad (30)$$

where, $Bn = An \exp\left(-\frac{En}{RT}\right)$

In order to account for the volumetric contraction due to reaction and hence, for the variation of superficial gas velocity along the reactor axis, a linear dependence of $\overline{U}_G$ on the syn-gas conversion was assumed in Model 1, in accordance with the models reported in literature. (Deckwer, 1980; Bukur, 1983; Kuo et al., 1983).

However, this relationship is valid only when axial mixing and convection in the liquid phase can be neglected and the stoichiometric coefficients do not vary with conversion. (Stern et al., 1985a) Since the latter condition is not valid, such a linear dependence of $\overline{U}_G$ on conversion of syn-gas is not satisfactory. In order to overcome this difficulty, an overall gas phase balance is established at constant reactor pressure.

$$-\theta_G \frac{d\overline{U}_G}{dz} + \sum_i \rho_i = 0 \qquad (31)$$

with the boundary condition, $\overline{U}_G = 1 \qquad @ \; z = 0$

(ii) Axial Dispersion in Gas and Liquid Phase:

With a view of relaxing the assumption of plug flow in the gas and the liquid phase and expressing the model equations in general terms, an axial dispersion model has been developed. All other assumptions remaining the same, the component mass balance equations are given by

Gas phase component balance,

$$\frac{\varepsilon_G}{Pe_G}\frac{d^2\theta_{G_i}}{dz^2} - \frac{d(\bar{U}_G\theta_{G_i})}{dz} - N_{G_i}(\theta_{G_i}-\theta_{L_i}) = 0 \qquad (32)$$

with the boundary conditions

$$\theta_{G_i} - \frac{\varepsilon_G}{Pe_G}\frac{d\theta_{G_i}}{dz} = \theta_{G_i}^{o} \qquad @\ z = 0 \qquad (33)$$

$$\frac{d\theta_{G_i}}{dz} = 0 \qquad @\ z = 1 \qquad (34)$$

The component balance in the liquid phase is given by

$$N_{G_i}\ m_i\ (\theta_{G_i}-\theta_{L_i}) + \frac{1}{Pe_L}\frac{d}{dz}\left[\varepsilon_L\ \frac{d\theta_{L_i}}{dz}\right] + \frac{m_i L\ C_{cat}(1-\varepsilon_G)}{C_{GH}^{o}\ U_G^{o}}\gamma_i = 0 \qquad (35)$$

where, γ_i represents the net rate of formation of any species i.

Incorporating the kinetic expression based on Ru/Al_2O_3 catalyst discussed earlier;

$$N_{G_i}\ m_i(\theta_{G_i}-\theta_{L_i}) + \frac{\varepsilon_L}{Pe_L}\frac{d^2\theta_{L_i}}{dz^2} + \left[\frac{m_i L\ C_{cat}(1-\varepsilon_G)C_{GHo}^{a_n+b_n-1}(RT)^{a_n+b_n}B_n}{U_G^{o}\ m_H^{a_n}\ m_{CO}^{b_n}}\right]\theta_{L_H}^{a_n}\theta_{L_{CO}}^{b_n} \qquad (36)$$

with the boundary conditions:

$$\frac{d\theta_{L_i}}{dz} = 0 \qquad @\ z = 0 \qquad (37)$$

$$\frac{d\theta_{L_i}}{dz} = 0 \qquad @\ z = 1 \qquad (38)$$

The variation of superficial gas velocity along the reactor axis is given by,

$$\theta_G \frac{d\bar{U}_G}{dz} + \sum_i N_{G_i} (\theta_{G_i} - \theta_{L_i}) = 0 \qquad (39)$$

In all the above equations, the following dimensionless groups were used,

$$Pe_G = \frac{U_G{}^o L}{D_G}\ ,\ N_{Gi} = \frac{K_{Li} a_L}{m_i U_G{}^o}$$

$$Pe_L = \frac{U_G{}^o L}{D_L}$$

The various physico-chemical properties and the hydrodynamic parameters involved in the model equations are estimated using correlations reported in the literature. These are incorporated in different subroutines and can be updated by the user, as and when required. A list of the correlations is given in Table I-B-2.

c. Numerical Solution

Depending upon the assumption made regarding the description of the gas and the liquid phase viz. plug flow or axial dispersion, the model

Table I-B-2

Correlations for the Estimation of Physico-Chemical and Hydrodynamic Properties used in BCSR Model 2

1. Slurry Density:

$$\rho_{SL} = V_{cat}\,\rho_{cat} + (1-V_{cat})\,\rho_L \qquad (gm/cm^3)$$

2. Liquid Density:

The liquid density is approximated to that of Gulf wax as reported by Albal (1983)

Temp (^oK)	Density (kg/m^3)
348	778.5
423	727.6
523	682.9

3. Volume fraction of solids:

$$V_{cat} = \frac{\rho_L W_{cat}}{\rho_{cat} - W_{cat}(\rho_{cat} - \rho_L)}$$

where
W_{cat} = catalyst loading = m_{cat}/m_{sus}

4. Solubility coefficients:

(Peter and Weinert, 1955)

The solubility coefficient for hydrocarbon species is approximated to that of C_5H_{10}

$m_H = 4.35^*$
$m_{CO} = 3.30$
$m_{H_2O} = 1.17$
$m_{cn} = 2.42$

*all @ 270°C

5. Gas phase holdup:

(Deckwer et al., 1980)

$$\varepsilon_G = 0.053 U_G^{1.1}$$

6. Gas-liquid mass transfer coefficient:

$$K_{LCO}\,\underline{a} = 0.05\ U_G$$

$$K_{LH}\,\underline{a} = K_{L_{CO}}\,\underline{a} \qquad \text{(Albal et al., 1983)}$$

$$K_{L_i}\,\underline{a} = K_{L_{CO}}\,\underline{a}\,\left[\frac{Di}{D_{CO}}\right]^{2/3} \qquad \text{(Calderbank, 1961)}$$

7. Gas phase diffusivities:

$D_{H_2O} = 1.24 \times 10^{-4}$ cm^2/sec (Reddy and Doraiswamy, 1967)

$D_{CO} = 3.2 \times 10^{-5}$ cm^2/sec (Zaidi et al., 1979)

$D_{C_5H_{10}} = 5 \times 10^{-4}$ cm^2/sec (Hayduk et al., 1973)

8. Gas phase dispersion coefficient:

(Towell and Ackerman, 1972)

$$D_G = 0.2\ d^2 U_G$$

9. Liquid phase dispersion coefficient:

(Deckwer, 1974)

$$D_L = 2.7 d^{1.4} U_G^{0.3}$$

equations obtained are different and have to be solved using different numerical techniques.

Thus, equations based on plug flow assumption are first order differential equations representing the gas phase component balance (Equation 22) and the total gas phase balance (Equation 31). However, the liquid phase component balance (Equation 24) is an algebraic equation. Furthermore, since the kinetic rate expression depends only on the concentrations of H_2 and CO in the liquid hase, one has to estimate Θ_{LH} and Θ_{LCO} before one can solve the gas phase balance. This is done by adopting a trial and error method to solve equation (24). The values of Θ_{LH} and Θ_{LCO} thus obtained, are used to solve the gas phase component balance and the total gas balance simultaneously, using the fourth order Runge-Kutta Verner method, available in the form of a package, DVERK, in the IMS Library.

Model equations incorporating the axial dispersion assumption constitute a boundary value problem with a set of second order differential equations both for the gas phase (Equation 32) and the liquid phase (Equation 35) component balances. A total of 18 second order differential equations are solved using the algorithm, COLSYS (Ascher et al., 1981). The algorithm uses the method of spline collocation at Gaussian points. The variation of superficial gas velocity along the reactor is established using the total gas balance equation.

d. Parameter Effects on Reactor Performance:

The program incorporating the axial dispersion assumption was used to study the effect of the operating parameters on the reactor performance viz. the syngas conversion and the H_2/CO usage ratio.

Effect of Inlet Gas Velocity on Conversion:

As observed in case of the BCSR Model 1, the syngas conversion falls

Table I-B-3

Kinetic Parameters for F-T Synthesis Over Ru/Al_2O_3 Catalyst

$$\gamma_{C_n} = A_n \exp\left(-\frac{En}{RT}\right) P_{H_2}{}^{a_n} P_{CO}{}^{b_n} \qquad n \leq 4$$

$$\gamma_{C_n} = \gamma_{C_4} \alpha^{n-4} \qquad n \geq 4$$

Carbon No.	A_n (mol/gm sec $(atm)^{a+b}$)	E_n (kcal/mol)	a_n	b_n
1	9.20×10^4	28	1.37	-0.84
2	6.70×10^4	27	0.66	-0.73
3	2.30×10^3	27	1.04	-0.35
4	0.97	20	1.11	-0.05

with an increase in the inlet superficial gas velocity (Fig. I-B-10). This effect may be attributed to the increased level of axial dispersion at higher operating velocities and a decreased residence time of the reactants within the reactor.

- Effect of Inlet H_2/CO Molar Ratio on Conversion:

Change in the inlet H_2/CO molar ratio can be brought about either by a change in the partial pressure of H_2 at constant CO inlet partial pressure or vice versa. Both these changes lead to an increase in the syngas conversion with an increase in the H_2/CO molar ratio at the inlet (Fig. I-B-11, I-B-12).

- Effect of Inlet H_2/CO Molar Ratio on the H_2/CO Usage Ratio:

Increase in the H_2/CO molar ratio at the inlet, either due to a change in the partial pressure of H_2 or CO, leads to an increase in the H_2/CO usage ratio as seen in Fig. I-B-13 and Fig. I-B-14.

Fluidized Bed Reactor

Fluidization is a technique of gas-solids contact in which a bed of solid particles is brought to a state of contained or uncontained motion by the gas flowing through the bed. As the velocity of a fluid through a packed bed is progressively increased, a stage is reached when the pressure-drop across the bed becomes equal to the weight of the solids. A bed in this state exhibits the properties of a fluid. As the velocity is further increased, the situation becomes similar to the introduction of a gas in a liquid. The additional gas flows through this gas-solid phase in the form of bubbles.

Beginning with the first large-scale use in catalytic cracking in 1942, the interest and effort centered on this technique has been phenomenal. Many other processes have been proposed, some of which actually reached the pilot plant stage and were then abandoned, while others progressed to full-scale

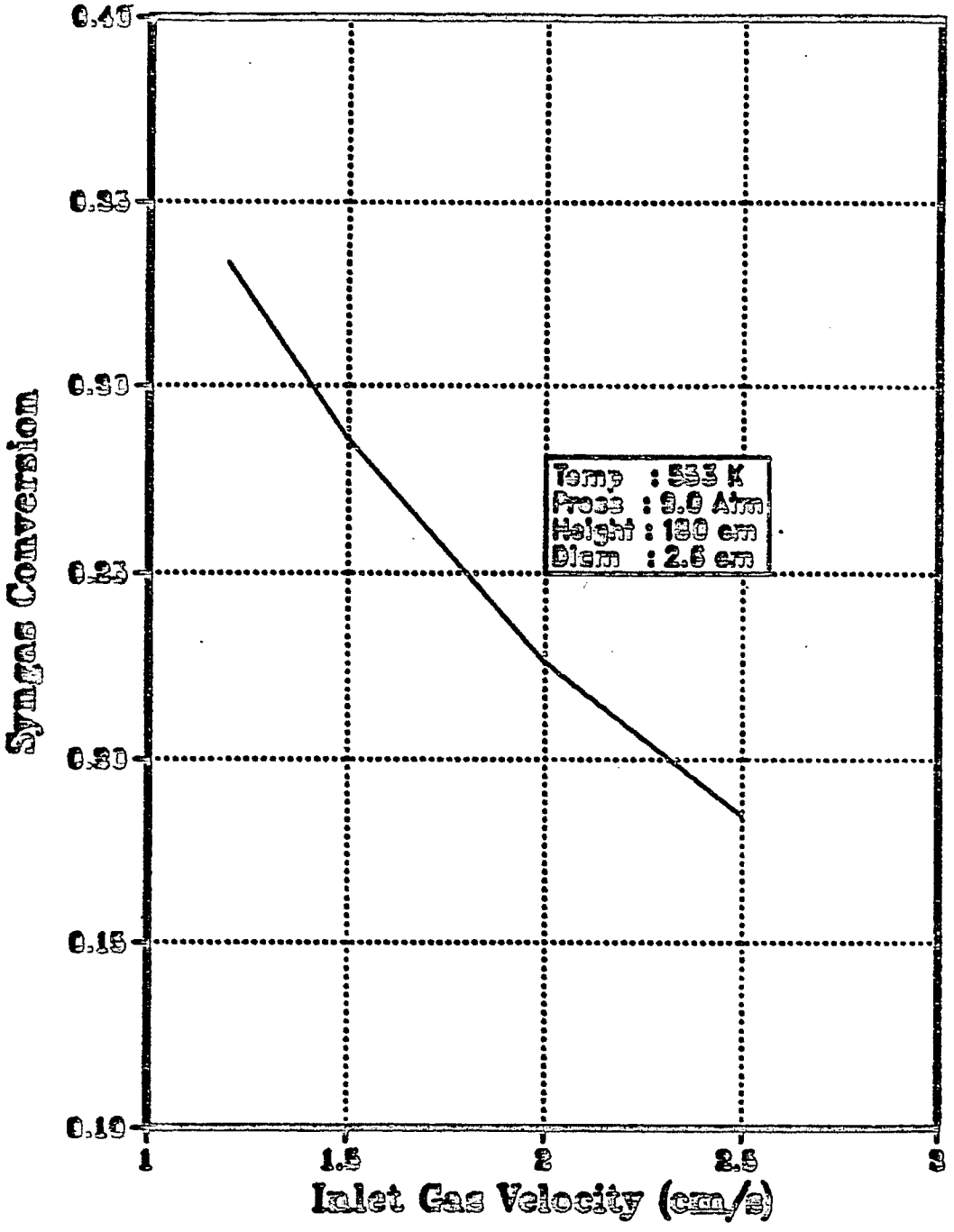

Figure I-B-10: Effect of Inlet Gas Velocity on Syngas Conversion

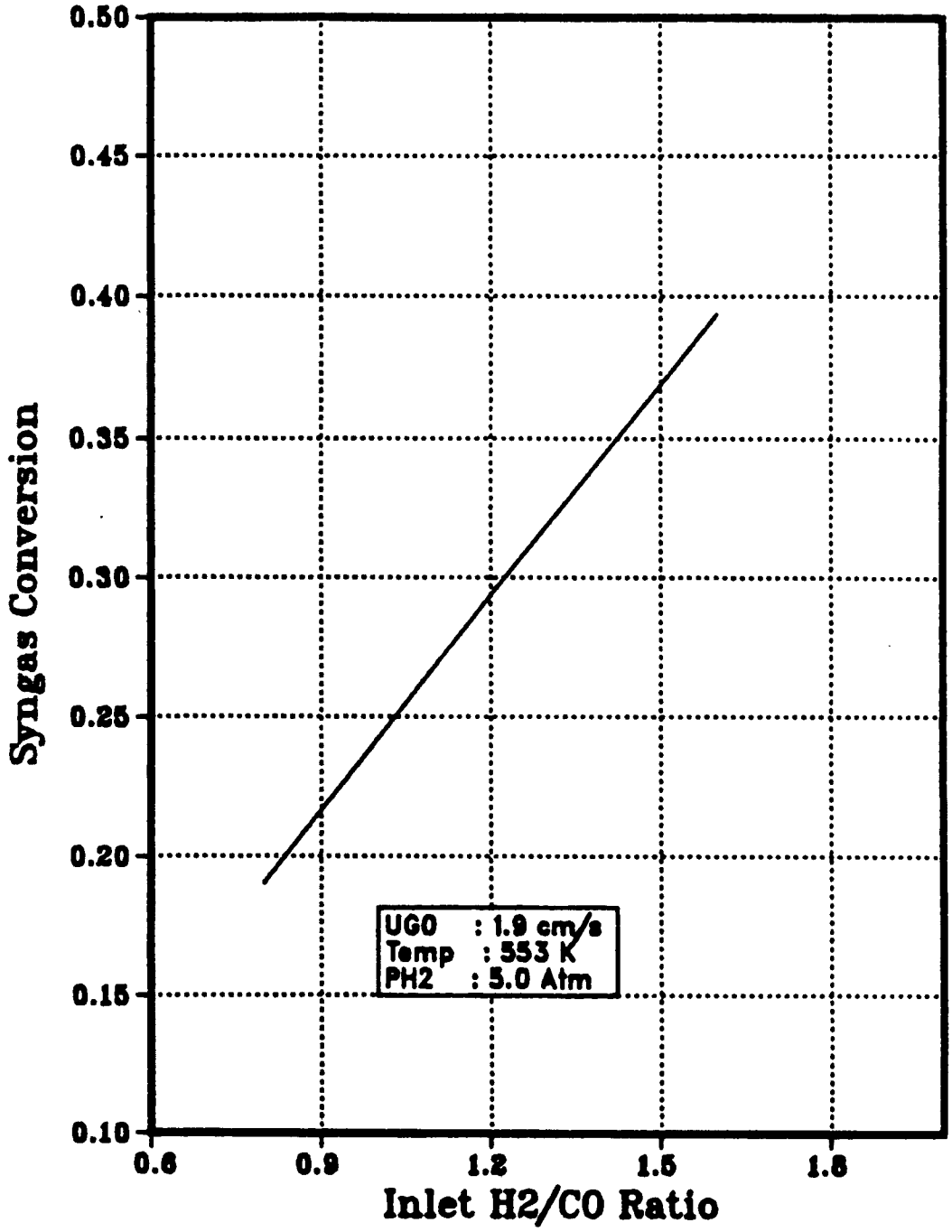

Figure I-B-11. Effect of Inlet Compositon on Syngas Conversion [P_{H_2} = 5]

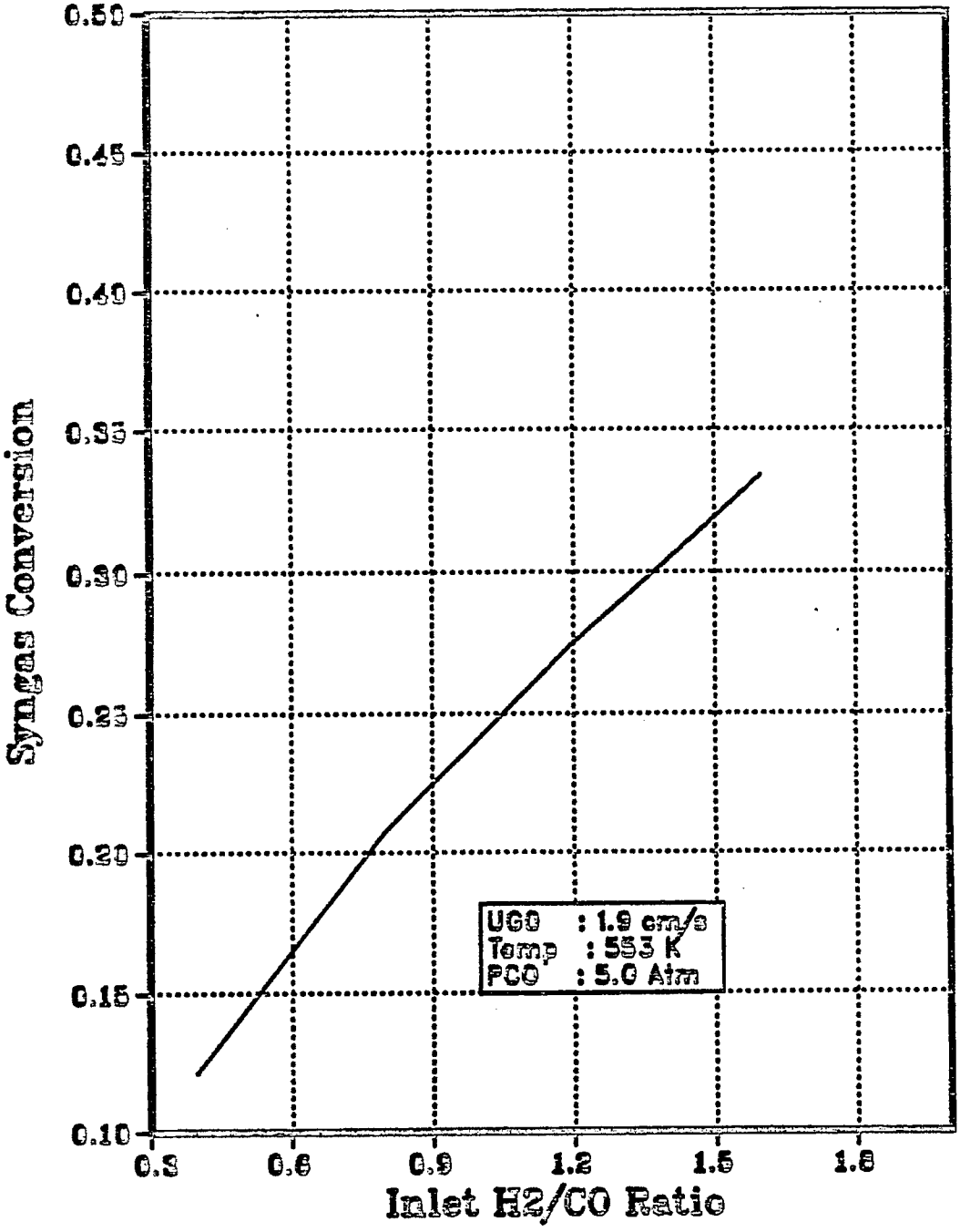

Figure I-B-12. Effect of Inlet Composition on Syngas Conversion [P_{CO} = 5]

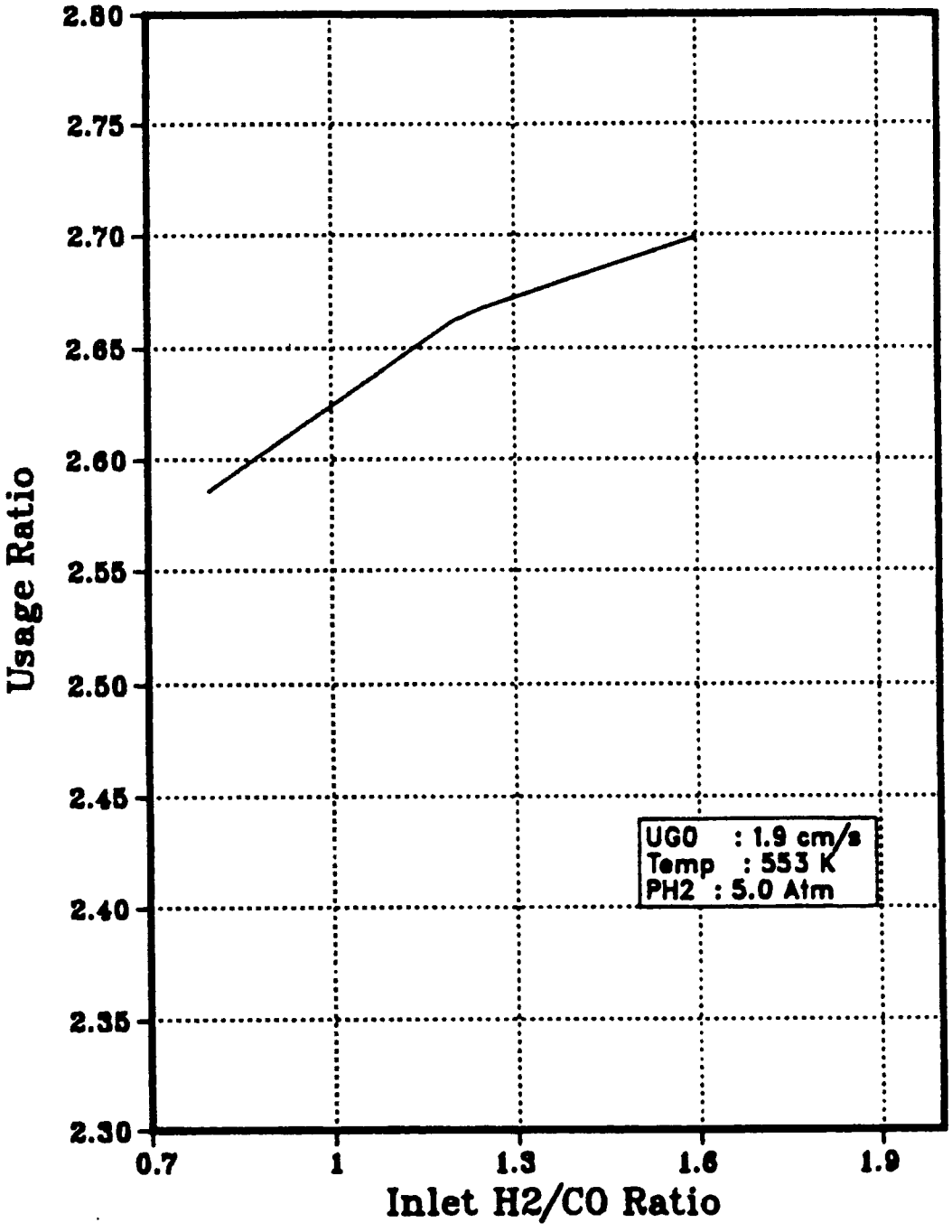

Figure I-B-13: Effect of Inlet Composition on Usage Ratio [P_{H_2}=5]

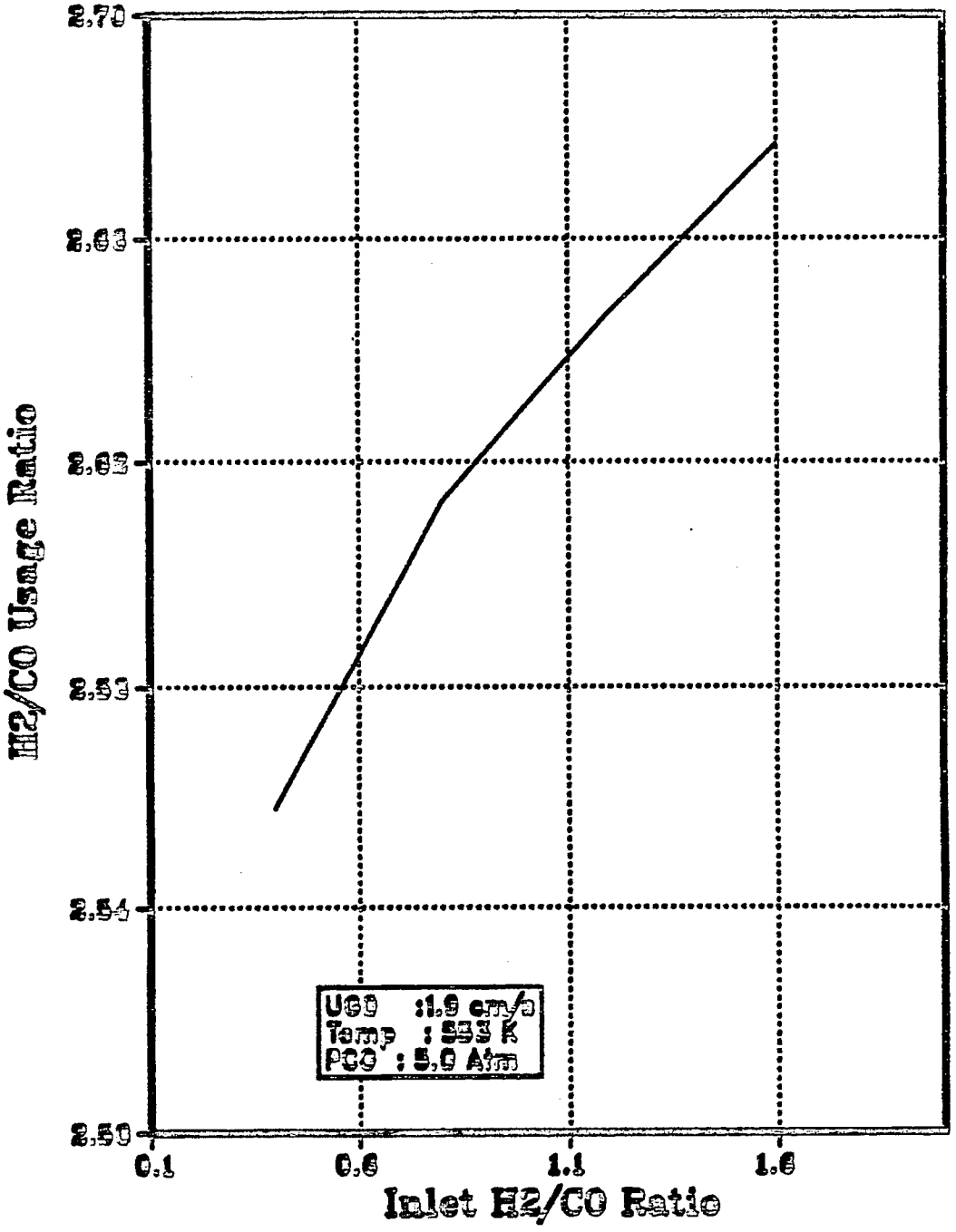

Figure I-B-14: Effect of Inlet Composition on Usage Ratio [P_{CO}=5]

plant stage and were then abandoned, while others progressed to full-scale plants like the catalytic reforming or the manufacture of acrylonitrile, phthalic anhydride and maleic anhydride (Rase, 1977).

Following the successful utilization of fluidized beds in catalytic cracking in the petroleum industry, the technique was also tried for F-T synthesis. However, due to the higher density of the iron catalyt used in F-T synthesis, factors such as the catalyst size and distribution, gas velocity and effective gas distribution become very critical. With a view of overcoming these difficulties, two basic types of units were tried viz., (i) fixed-fluidized bed (FFB) in which the catalyst bed remains stationary with gas passing upward through it, (ii) the circulating fluidized bed (CFB) in which the catalyst is entrained in the fast moving gas stream. The Kellogg Company (USA) developed the CFB and this was scaled up from their 10 cm ID reactor the 220 cm ID commercial unit at Sasol I. After several mechanical and process modifications the system which is now known as the "Sasol Synthol Process" can reliably achieve satisfactory syn-gas conversion. The reactor used at Sasol is as shown in Figure I-B-15. The fresh feed and the recycle gases are fed in at the bottom where it meets a down flowing stream of hot, finely divided catalyst. The combined gas and catalyst stream sweeps through the reaction zone. The catalyst and the gas disengage in the wide settling hopper at the reactor exit (Dry, 1981).

One of the major advantages in using a fluidized bed reactor for F-T synthesis is its excellent heat transfer characteristics, which may be attributed to the high solids surface area along with the continuous and rapid particle movements to and from the heat transfer surface. The high degree of turbulence present in the reactor effectively eliminates axial and radial temperature gradients, resulting in an essentially isothermal condition.

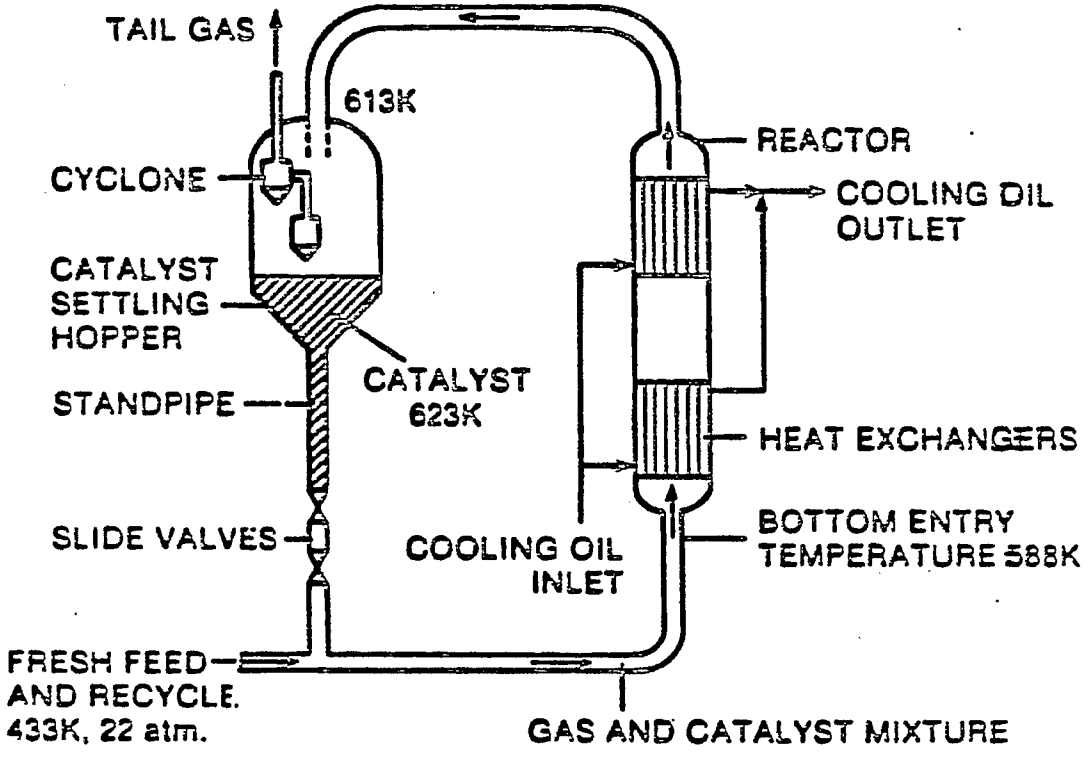

Figure I-B-15. Sasol Synthol Reactor

Furthermore, one of the major advantages accrued due to the use of a fluidized bed reactor is the allowance for continuous recirculation of solids which is necessary especially in cases where the reaction may lead to a rapid deactivation of the catalyst.

A considerable volume of literature has been accumulated over the last 20 years on several aspects of fluidization. These have been summarized in several books (Davidson and Harrison, 1963; Kunii and and Levenspiel, 1969; and Keairns, 1976). As mentioned earlier, all the gas in excess of that required for the onset of fluidization travels through the bed in the form of bubbles, thus giving rise to the two-phase concept whereby we have a bubble phase and a continuous gas-solid emulsion phase. This concept, commonly referred to as the "two-phase theory," was first proposed by Toomey and Johnstone (1952). Based on this concept, several models were proposed to explain the performance of a fluidized bed (Johnstone et al. 1955); (Massimilla and Johnstone, 1961), etc. All these models assumed that gas is continuously interchanged between the bubble and dense phases, the fluid bed efficiency was expressed in terms of an exchange parameter, and that the gas in the dense phase was either in plug flow or perfectly mixed with the bubble phase in plug flow.

Later, models based on the mechanics of bubbles in a spontaneously bubbling gas-fluidized bed were developed (Patridge and Rowe, 1966; Davidson and Harrison, 1963). However, these models based on the two phase theory, do not account for the gas backmixing, a concept which has long been recognized in beds fluidized with gas. The upward flow of solids with the bubbles leads to a downflow of solids in the remainder of the bed, and if this downflow were sufficiently rapid, a very simple mechanism of gas backmixing arose (Stephen et al., 1967). Based on this mechanism, counter-current flow models have been

developed to predict the performance of a fluidized bed reactor (Latham et al., 1968, Kunii and Levenspiel, 1968). With a view of simplifying the solution of the model equations, several assumptions were made which were latter on relaxed so as to propose a generalized model (Fryer and Potter, 1972).

In the present work, use is made of this generalized countercurrent flow model to describe the performance of the fluidized bed reactor used for F-T synthesis. Similar to the models developed for BCSR, two different models have been developed:

FBR MODEL 1

The model equations incorporating the counter-current backmixing phenomenon observed in fluidized bed reactors operated at high superficial gas velocity are based on the following assumptions:

a. Model Assumptions:

i) There is no temperature change along the reactor axis, i.e., isothermal operation.

ii) The bubbles are assumed to be of uniform size all through the reactor. Interaction between bubbles most commonly lead to coalescence so that bubble size increases with height while the number decreases. During and prior to coalescence bubbles distort their shape and velocity changes occur. The little information available from theory, research experiments, or industrial experience to enable bubble size, number, and distribution to be predicted in a given situation has been a major obstacle to the application of chemical reactor models. The performance of a fluidized bed thus strongly depends on the bubble size but a stable bubble size that would eventually attained is assumed.

bubble size but a stable bubble size that would be eventually attained is assumed.

iii) The bubbles are uniformly distributed throughout the reactor cross section.

iv) Associated with every bubble is a wake of solids which flows upwards behind the bubbles but flows downwards in the rest of the emulsion.

v) The cloud volume is neglected or rather lumped with the wake volume.

vi) The amount of solids present in the bubble phase is negligible thus leading to a minimal contact of the reactant gas with the solids in the bubble phase. This is also based on the assumption that the catalyst is not highly active, leading to a negligible reaction in the bubble phase.

vii) The emulstion stays at minimum fluidizing conditions, thus the relative velocities of gas and solid remain unchanged.

viii) Gas exchange along the reactor axis occurs in two stages, viz. bubble phase to cloud-wake phase and cloud-wake phase to particulate phase.

ix) The rate of reaction is assumed to be first order in H_2 concentration (Dry, 1976; Atwood and Bennett, 1973) and occurs in the presence of particles in the cloud-wake and in the particulate phase.

$$\gamma_{CW} = K_H C_{CH}$$

$$\gamma_P = K_H C_{PH}$$

The rate constant used is for F-T synthesis over commercial nitrided fused Fe-catalyst. (Atwood and Bennett, 1979). The use of a first order kinetic expression is not truly satisfactory for industrial scale reactors which

operate at integral conversions. A more general kinetic expression would be of the form,

$$\gamma = \frac{K_H C_{H_2} C_{CO}}{C_{CO} + bC_{H_2O}}$$

But in case of a high shift activity of the catalyst the inhibiting action of product water becomes negligible and a first order dependence on C_{H_2} is obtained. The product distribution reported by Atwood and Bennett (1979) exhibits an inhibition due to water only at highest conversions and very high temperatures of operation. Thus, the use of first order kinetics may not be very satisfactory and may overestimate the reactor performance.

x) The volumetric contraction due to reaction is accounted for using the concept introduced by Levenspiel (1972) and as used by Deckwer et al. (1980).

$$U_G = U_G^o (1 + \alpha X_{CO+H_2}) \text{ where, } \alpha = -0.5 \text{ to } -0.6$$

xi) The unknown stoichiometry of the F-T reaction is accounted for by using the concept of CO/H_2 usage ratio as used by Deckwer et al. (1980).

$$H_2 + UCO \rightarrow \text{Products}$$

b. Model Equations:

The equations describing the material balance in the various phases of a fluidized bed reactor are based on the representation of an elemental volume as shown in Figure I-B-16. The superficial fluidizing velocity through

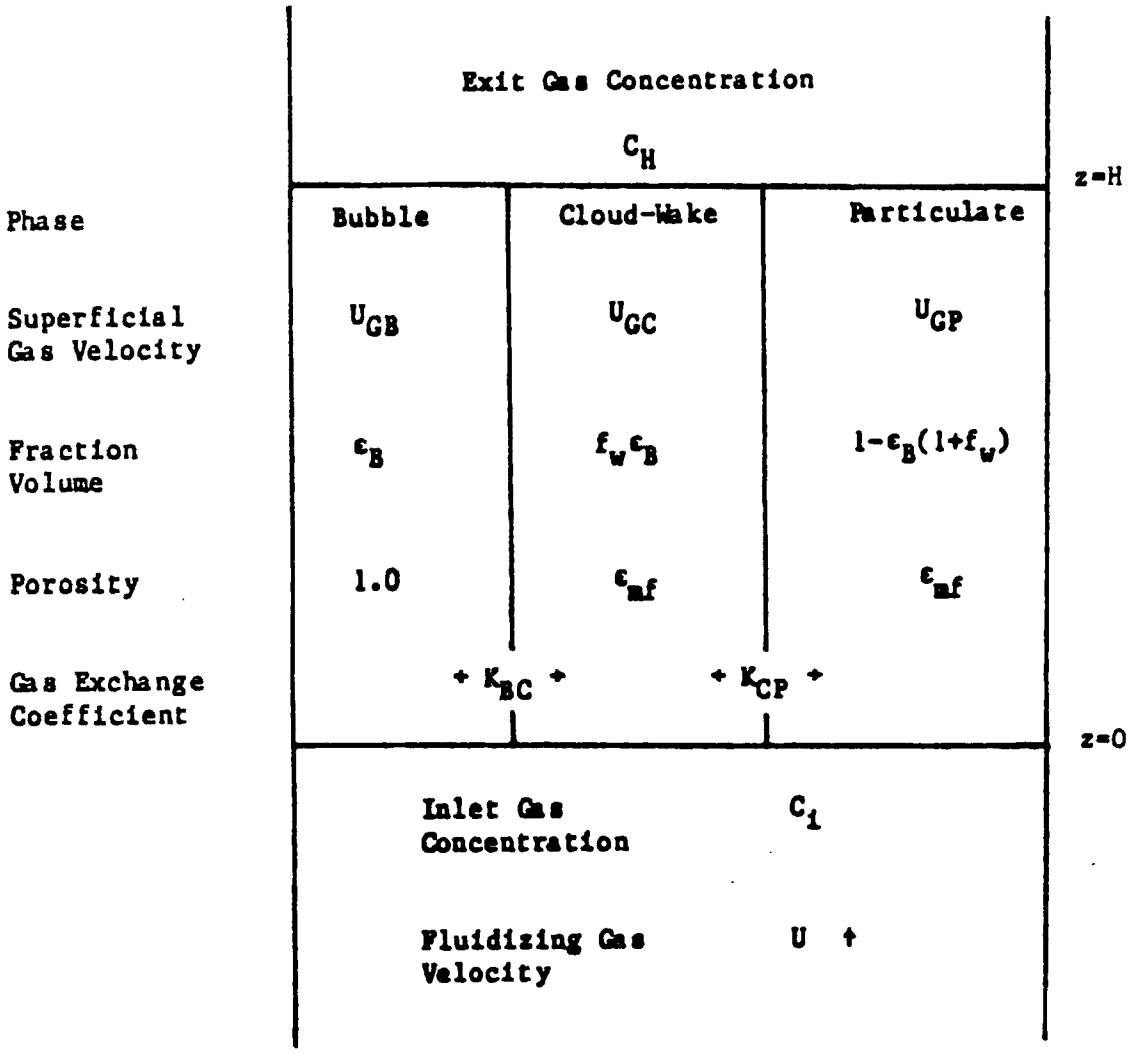

Figure I-B-16. Representation of a Fluidized Bed Reactor

the reactor is given by,

$$U_G = U_{GB} + U_{GP} + U_{GC} \tag{40}$$

Since the bubble phase and the cloud-wake phase rise together, the cloud-phase velocity is inter-related with the bubble phase velocity,

$$U_{GC} = f_w \varepsilon_o U_{GB} \tag{41}$$

The superficial velocity of solids carried up in the bubble wakes is $U_{GB} f_w (1-\varepsilon_o)$, which would also be the velocity of solids in the particulate phase, but in the downward direction. Since, the relative velocity of the gas to solids in the particulate phase remains unchanged, it can be obtained from the conditions at incipient fluidization,

$$\frac{U_{GP}}{[1 - \varepsilon_B (1 + f_w)]\ \varepsilon_o} + \frac{U_{GB}\ f_w\ (1 - \varepsilon_o)}{[1 - \varepsilon_B (1 + f_w)]\ (1 - \varepsilon_o)} = \frac{U_o}{\varepsilon_o} \tag{42}$$

Using Equations 40 and 42, the superficial gas velocities in the bubble phase and the particulate phases are given by,

$$U_{GB} = U_G - U_o\ [1 - \varepsilon_B\ (1 + f_w)] \tag{43}$$

$$U_{GP} = U_o\ [1 - \varepsilon_B\ (1 + f_w)]\ [1 + \varepsilon_o f_w] - U_G f_w \varepsilon_o \tag{44}$$

Counter-current backmixing of gas is present when the velocity in the particulate phase (U_{GP}) is negative, a phenomenon observed when the total superficial gas velocity exceeds a critical value given by,

$$\frac{U_{cr}}{U_o} = \left[1 + \frac{1}{\varepsilon_o f_w}\right] \left[1 - \varepsilon_B (1 + f_w)\right] \tag{45}$$

Having evaluated the superficial gas velocities in each phase, one can establish a material balance on reactant gas over the differential height in each of the phases, (Figure I-B-16). Use is made of the following dimensionless variables in developing the material balance equations:

$$C_{1H} = \frac{C_{BH}}{C_{HO}}, \quad C_{2H} = \frac{C_{CH}}{C_{HO}}, \quad C_{3H} = \frac{C_{PH}}{C_{HO}}, \quad z = \frac{x}{H} \tag{46}$$

Thus, for the bubble phase,

$$\frac{dC_{1H}}{dz} = A_1 C_{1H} + A_2 C_{2H} \tag{47}$$

where

$$A_1 = \frac{-K_{BC}{}^H \varepsilon_B}{U_{GB}}, \quad A_2 = \frac{K_{BC}{}^H \varepsilon_B}{U_{GB}} \tag{48}$$

with the boundary condition, $C_{1H} = 1$, @ $z = 0$, since all the bubble gas is derived from the incoming gas.

For the cloud-wake phase,

$$\frac{dC_{2H}}{dz} = A_3 C_{1H} + A_4 C_{2H} + A_5 C_{3H} \tag{49}$$

where

$$A_3 = \frac{K_{BC}{}^H \varepsilon_B}{U_{GC}}, \quad A_4 = \frac{-H \varepsilon_B (K_{BC} + K_{CP} + K_H f_w)}{U_{GC}} \tag{50}$$

$$A_5 = \frac{K_{CP}{}^H \varepsilon_B}{U_{GC}}$$

with the boundary condition,

$$C_{2H} = \left(\frac{U - U_{GB}}{U_{GC}}\right) + \left[1 - \left(\frac{U - U_{GB}}{U_{GC}}\right)\right] C_{3H} \qquad @\ z = 0 \qquad (51)$$

since the cloud-wake gas is derived from the remainder of the incoming gas and the downflowing particulate phase gas, under backmixing conditions.

For the particulate phase,

$$\frac{dC_{3H}}{dz} = A_6 C_{2H} + A_7 C_{3H} \qquad (52)$$

where,

$$A_6 = \frac{K_{CP}H\ \varepsilon_B}{U_{GP}} \qquad (53)$$

$$A_7 = \frac{-(K_{CP}H\ \varepsilon_B + K_H H\ (1 - \varepsilon_B\ (1 + f_w)))}{U_{GP}}$$

with the boundary condition, $C_{2H} = C_{3H}$ @ $z = 1$, since the gas leaving at the top of the bed is considered to be made up of all the bubble gas and some of the cloud-wake gas, with the remainder of the cloud-wake providing the downflowing gas in the particulate phase.

In developing the material balance equations, a number of system parameters such as the transfer coefficients, volume fractions, etc., are involved. These parameters are evaluated using expressions based on bubble mechanics and the phenomenon of gas exchange between various phases. A list of various expressions and correlations used is given in Table I-B-4. The average gas concentration at any point in the reactor in proportion to the fractions of the phases present is given by,

$$C_{av_H} = C_{HO}\ [\varepsilon_B C_{1H} + f_w \varepsilon_B C_{2H} + (1 - \varepsilon_B\ (1 + f_w))\ C_{3H}] \qquad (54)$$

Table I-B-4

Correlations and Expressions used to Evaluate System Parameters in Fluidized Bed Reactor

1. Gas exchange coefficients:

(Kunii and Levenspiel, 1968)

$$K_{BC} = 4.5 \left(\frac{U_o}{D_e}\right) + 5.85 \left(\frac{g^{1/4} D_G^{1/2}}{D_e^{5/4}}\right)$$

$$K_{CP} = 6.78 \left(\frac{\varepsilon_o D_G U_A}{D_e^3}\right)^{1/2}$$

2. Bubble rise velocity:

$$U_A = U_G - U_o + 0.711 (g D_e)^{1/2}$$

3. Bubble volume fraction:

$$\varepsilon_B = \frac{U_{GB}}{U_A}$$

4. Ratio of wake volume to bubble volume:

$$f_w = 1 \qquad \text{for } \varepsilon_B < 1/3$$

$$f_w = \frac{1 - \varepsilon_B}{2\ \varepsilon_B} \qquad \text{for } \varepsilon_B > 1/3$$

$$f_w = \frac{1 - \varepsilon_B}{2\ \varepsilon_B} \text{ for } \varepsilon_B > 1/3$$

5. Velocity at inicipient fluidization:

$$U_{mf} = \frac{\varepsilon_{mf}^3}{5\ (1 - \varepsilon_{mf})} \frac{(\rho_s - \rho_f)\ g}{s^2 \mu}$$

for, $\varepsilon_{mf} = 0.4$ and spherical particles,

$$U_{mf} = 0.00059 \frac{d^2\ (\rho_s - \rho_f)\ g}{\mu}$$

6. Kinetic Parameters:

(Atwood and Bennett, 1979)

$$\gamma = \frac{K\ C_{H_2}\ C_{CO}}{C_{CO} + b\ C_{H_2O}}$$

under the assumption of high shift activity,

$$\gamma_{CO} = KC_{H_2}$$

and $\gamma_{H_2} = K_H C_{H_2}$, $K_H = \frac{K}{U}$

$$K = A \exp\left(\frac{-E_A}{RT}\right)$$

where, $E_A = 20.313$ kcal/gmol

$$A = 5.807 \times 10^9 \text{ hr}^{-1}$$

and the exit gas concentration is given by,

$$C_{EH} = C_{HO} \left[\left(\frac{U_{GB}}{U_G}\right) C_{1H} + \left(1 - \frac{U_{GB}}{U_G}\right) C_{2H}\right] \qquad (55)$$

Based on the bubble phase concentration of hydrogen, the conversion is obtained from the expression,

$$X_H = \frac{U_G^o C_{HO} - U_G C_{BH}}{U_G^o C_{HO}} \qquad (56)$$

and the syn-gas conversion is obtained from the reaction stoichiometry as defined by Deckwer et al. (1980).

$$X_{CO+H_2} = \left(\frac{1 + U}{1 + I}\right) X_H \qquad (57)$$

The above equations which constitute a bubbling bed model describe the performance of a fluidized bed reactor with no catalyst re-circulation. However, these equations can also be used for a circulating fluidized bed, with a slight modification in the expression for the bubble rise velocity U_A in Table I-B-4. This modification accounts for the effect of the solids velocity within the reactor on the bubble rise velocity. Accordingly,

$$U_A = U_G - U_o + 0.711 (g D_e)^{1/2} \pm U_s \qquad (58)$$

where, U_s is the solids velocity, being negative in the case of countercurrent flow and positive for co-current flow. The value of U_s is either decided from the rate of de-activation of the catalyst (e.g., in case of catalytic cracking) or may be a design parameter, obtained from (Doraiswamy and Sharma,

1984)

$$U_s = \frac{F_s}{(1 - f_B)\ \rho_s A_c} \qquad (59)$$

As the superficial gas velocity is progressively increased beyond that needed for bubbling, a point is reached where there is a sharp drop in the bed density over a narrow velocity range due to excessive carryover. In this regime, commonly called as the turbulent regime, it is necessary to feed the solids into the bed at the same rate at which they are removed at the top, in order to maintain the upper level of solids at a constant position. For velocities greater than a transition value, the fluid bed density is however, a strong function of the rate of solids fed in at the bottom of the bed. Fluidization under this regime is referred to as fast fluidization. This process of fast fluidization has not been fully explored, and information available is restricted to the use of fine particles. However, the use of high gas velocities employed make it possible to achieve better gas-solids contact and thus increase the reactor capacity.

In the present report, however, model equations describing the bubbling bed fluidized reactor have been analyzed.

c. Numerical Solution:

The mass balance equations in the bubble phase, the cloud-wake phase and the particulate phase (eqn. 47,49,52) along with their boundary conditions constitute a two point boundary value problem, which is solved using the algorithm, COLSYS. (Ascher et al., 1981). This algorithm uses the method of spline collocation at Gaussian points.

d. Parameter Effect on Reactor Performance

The kinetic expression used, viz. a first order dependence on H_2

concentration is quite simplistic and would describe F-T synthesis over a catalyst with a high shift activity such as Fe. The kinetic parameters used in the present case are those reported for nitrided iron catalyst (Atwood and Bennett, 1979). Nitrided iron catalysts for the F-T synthesis were developed at the Bureau of Mines. From the recent tests of F-T synthesis over commercially-available catalysts, Borghard and Bennett (1979) concluded that "nitrided fused iron and cobalt-silica catalysts look most promising". Nitrided iron catalysts are active and durable and have an unusual selectivity. They do not produce significant amounts of wax, which should be advantageous in situations where gasoline is the desired product. The low yield of wax permits operation of nitrided iron in fluidized fixed-bed or entrained reactors at lower temperatures as against conventional reduced iron catalysts which must be operated at about 325°C to prevent formation of higher hydrocarbons that leads to agglomeration of the fluidized particles. (Anderson, 1980). Furthermore, as indicated earlier, the inhibition of reaction rate due to formation of water becomes pronounced at higher temperatures, typical of reduced Fe catalyst. However, the use of a non-linear rate expression incorporating this effect would represent the phenomena more accurately as against the first order expression used here.

- Effect of Inlet Gas Velocity on Conversion.

The synthesis gas conversion drops with an increase in the inlet superficial gas velocity as shown in Figure. I-B-17. This may be attributed to the decrease in the residence time. However, this effect is

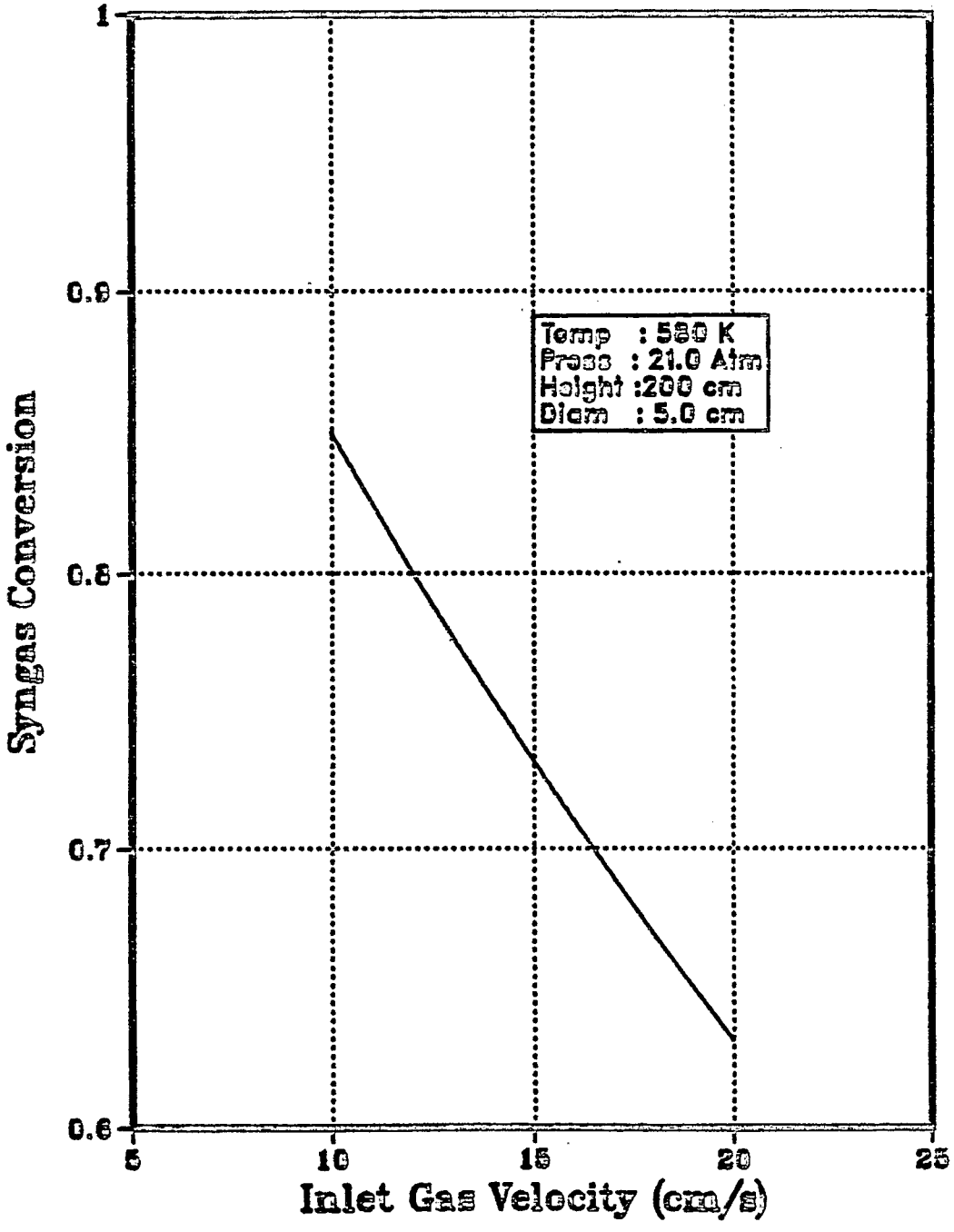

Figure I-B-17. Effect of Inlet Gas Velocity on Syngas Conversion [FBR]

not pronounced for velocities significantly higher than the velocity at minimum fluidization. The variation of STY with velocity is as shown in Fig. I-B-18.

. Effect of Operating Temperature on Conversion.

Increase in the operating temperature leads to an increase in the syngas conversion as seen in Figure I-B-19. However, at higher temperatures, the inhibition due to the water formed would become significant and hence the performance cannot be accounted for using a first order kinetic expression.

. Effect of Bubble Diameter on Conversion.

The conversion obtainable in a fluidized bed reactor drops with an increase in the bubble diameter (Figure I-B-20). This calls for the use of a stable bubble diameter under the operating conditions. Due to the lack of availability of data on bubble diameter, a suitable estimate of the bubble size was used in the simulator.

FBR Model 2:

With a view of describing the product distribution obtained during F-T synthesis in a fluidized bed reactor, use is made of the kinetic expression proposed by Stern et al. (1985b) for Ru/Al_2O_3 catalyst and as used in BSCR MODEL 2. The mass balance equations for the reactant and the product species for a fluidized bed reactor are based on the following assumptions.

a. Model assumptions:

i) Reaction rate expression for F-T synthesis over Ru/Al_2O_3 catalyst is assumed.

ii) Gas exchange coefficients for the transfer from one phase to another of all the species is assumed to be same. (Levenspiel, 1978).

iii) All other assumptions regarding the gas flow through the various phases are the same as described in FBR.MODEL 1.

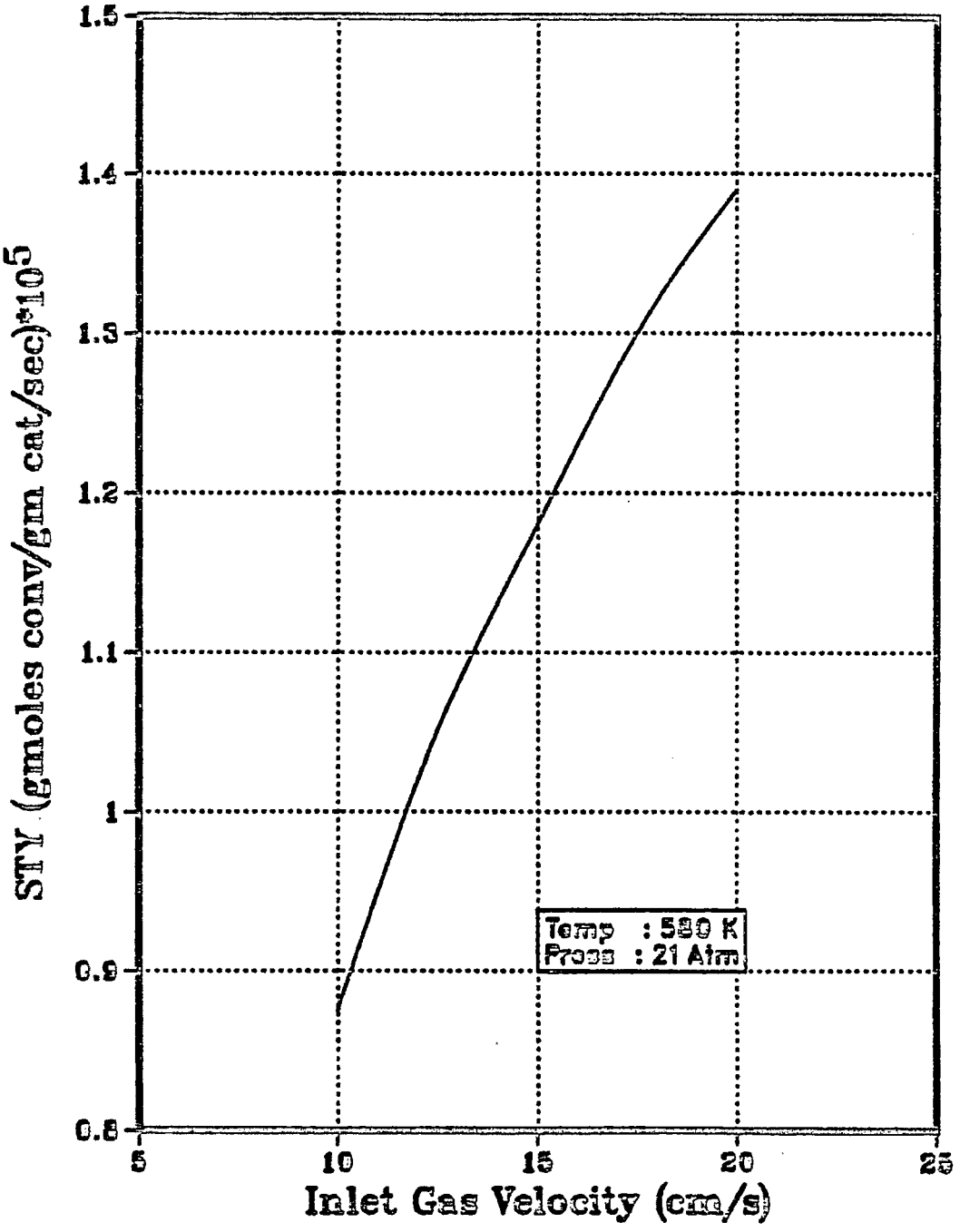

Figure I-B-18: Variation of STY with Inlet Gas Velocity (FBR)

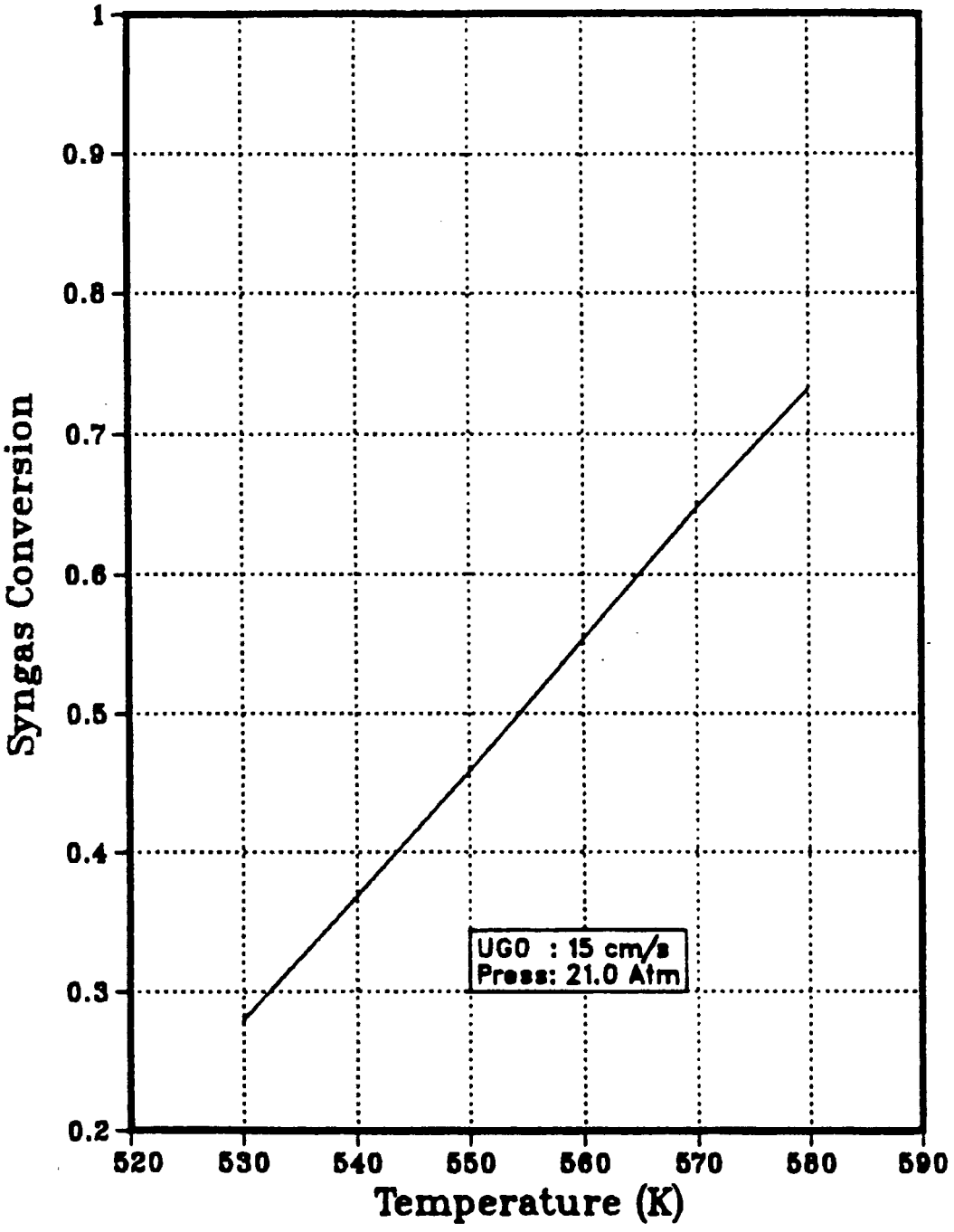

Figure I-B-19: Variation of Syngas Conversion with Temperature (FBR)

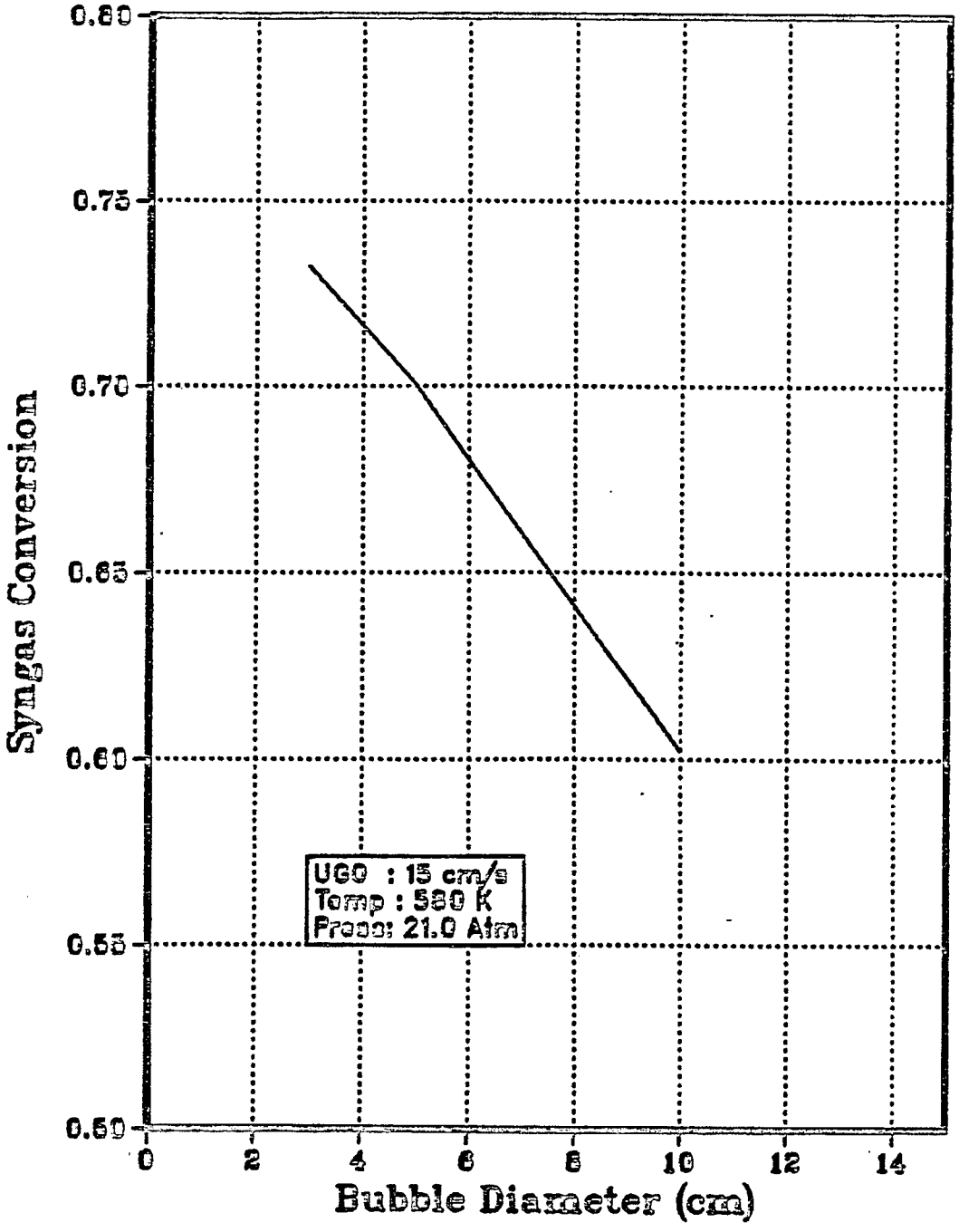

Figure I-B-20: Variation of Syngas Conversion with Bubble Diameter (FBR)

b. Model Equations:

The mass balance equations for each species in the bubble, the cloud-wake and the particulate phase have been developed with reference to the representation of the fluidized bed reactor as shown in Figure I-B-16.

The kinetic expression used in quantifying the contribution due to chemical reaction is a power law model (Stern et al., 1985b)

$$\gamma_{C_n} = A_n \exp\left(-\frac{En}{RT}\right) P_{H_2}^{a_n} P_{CO}^{b_n}$$

$$\gamma_{C_n} = B_n C_H^{a_n} C_{CO}^{b_n} \qquad \text{for } n = 1,2,3,4$$

where, $$B_n = \rho_{cat} A_n (RT)^{a_n+b_n} \exp\left(-\frac{En}{RT}\right)$$

$$\gamma_{C_n} = \alpha^{n-4} \gamma_{C_4} \qquad \text{for } n > 4$$

where, α represents the chain growth probability factor.

Equations representing component mass balance in the various phases are as given below:

Bubble Phase:

$$-\frac{d C_{B_i}}{dh} = \frac{K_{BC} (C_{B_i} - C_{C_i}) \varepsilon_B}{U_{GB}} \qquad (60)$$

$$-\frac{dC_{C_i}}{dh} = \frac{K_{CP} (C_{C_i} - C_{P_i}) \varepsilon_B + K_{BC} (C_{C_i} - C_{B_i}) \varepsilon_B + f_w \varepsilon_B R_{C_i} (1 - \varepsilon_{mf})}{U_{GP}} \qquad (61)$$

$$-\frac{dC_{P_i}}{dh} = \frac{K_{CP}(C_{P_i} - C_{C_i})\,\varepsilon_B + [1 - \varepsilon_B\,(1 + fw)]\,R_{P_i}\,(1 - \varepsilon_{mf})}{U_{GP}} \tag{62}$$

with the respective boundary conditions,

$$C_{B_i} = C_{io} \quad @\ h = 0 \tag{63}$$

$$C_{C_i} = \left(\frac{U_G - U_{GB}}{U_{GC}}\right) C_{io} + \left(1 - \frac{U_G - U_{GB}}{U_{GC}}\right) C_{P_i} \quad @\ h = 0 \tag{64}$$

$$C_{C_i} = C_{P_i} \quad @\ h = 1 \tag{65}$$

R_{C_i} and R_{P_i} represent the net depletion of the species in the cloud-wake and the particulate phases due to chemical reaction. The expressions for R_{C_i} and R_{P_i} for various species is as given below:

Carbon Monoxide:

$$R_{C_{CO}} = \sum_{n=1}^{3} n\,B_n\,C_{C_H}^{a_n}\,C_{C_{CO}}^{b_n} + B_4\,C_{C_H}^{a_4}\,C_{C_{CO}}^{b_4} \sum_{4}^{\infty} n\,\alpha^{n-4} \tag{66}$$

$$R_{P_{CO}} = \sum_{n=1}^{3} n\,B_n\,C_{P_H}^{a_n}\,C_{P_{CO}}^{b_n} + B_4\,C_{P_H}^{a_4} \sum_{4}^{\infty} n\,\alpha^{n-4} \tag{67}$$

Hydrogen:

$$R_{C_H} = \sum_{n=1}^{3} (2n+1)\, B_n\, C_{C_H}^{a_n}\, C_{C_{CO}}^{b_n} + B_4\, C_{C_H}^{a_4}\, C_{C_{CO}}^{b_4} \sum_{4}^{\infty} (2n+1)\, \alpha^{n-4} \qquad (68)$$

$$R_{P_H} = \sum_{n=1}^{3} (2n+1)\, B_n\, C_{P_H}^{a_n}\, C_{P_{CO}}^{b_n} + B_4\, C_{C_H}^{a_4}\, C_{C_{CO}}^{b_4} \sum_{4}^{\infty} (2n+1)\, \alpha^{n-4} \qquad (69)$$

Water:

$$R_{C_{H_2O}} = - R_{C_{CO}} \qquad (70)$$

$$R_{P_{H_2O}} = - R_{P_{CO}} \qquad (71)$$

Hydrocarbons:

$$R_{C_{cn}} = - B_n\, C_{C_H}^{a_n}\, C_{C_{CO}}^{b_n} \qquad \text{for } n = 1,2,3 \qquad (72)$$

$$R_{P_{cn}} = - B_n\, C_{P_H}^{a_n}\, C_{P_{CO}}^{b_n} \qquad \text{for } n=1,2,3 \qquad (73)$$

$$R_{C_{cn}} = - B_4\, C_{C_H}^{a_4}\, C_{C_{CO}}^{b_4}\, \alpha^{n-4} \qquad \text{for } n > 4 \qquad (74)$$

$$R_{P_{cn}} = - B_4\, C_{P_H}^{a_4}\, C_{P_{CO}}^{b_4}\, \alpha^{n-4} \qquad \text{for } n > 4 \qquad (75)$$

Where,

$$B_n = [An \exp(\frac{-En}{RT})]\, \rho_{cat} \cdot (RT)^{an+bn}$$

All the above mass balance equations are based on the stoichiometric equation,

$$n\ CO + (2n+1)\ H_2 \rightarrow C_nH_{2n+2} + n\ H_2O$$

The expressions used to evaluate the superficial gas velocities in the bubble, the cloud-wake and the particulate phase, the transfer coefficients and all other system parameters are the same as used in the FBR Model 1 and as indicated in Table I-B-4.

c. Numerical Solution:

The mass balance equations for each species in each of the phases (eqns. 60,61,62) together constitute a two point boundary value problem. A set of 30, first order differential equations is solved using the method of spline collocation, available in the form of a software package, COLSYS (Ascher et al., 1981). Certain modifications had to be made within the code to handle a set of 30 differential equations. For details, one should refer to the paper by Ascher et al., (1981).

FIXED BED REACTOR

In its most basic form, a fixed bed reactor consists of a cylindrical tube filled with catalyst pellets. Reactants flow through the catalyst bed and are converted into products.

Fixed bed reactors may be regarded as the workhorse of the chemical industry with respect to the number of reactors employed and the economic value of materials produced. Ammonia synthesis, sulphuric acid production, nitric acid production are only a few of the extremely large tonnage processes that make extensive use of various forms of fixed bed reactors. A fixed bed reactor has many unique and valuable advantages relative to the other reactor types. One of its prime attributes is its simplicity, with the attendant consequences of low costs for construction, operation and maintenance.

However, heat transfer to or from a large fixed bed of catalyst often represents a significant problem. A variety of operating techniques can be used to facilitate control over the bed temperature. Furthermore, if the catalyst deactivation rate is sufficiently rapid, costs associated with the catalyst regeneration or replacement may render the entire process unattractive from a commercial standpoint.

The use of fixed bed reactors for F-T synthesis was made by the original German industries of 1936. The catalyst was packed between perpendicular parallel metal plates spaced 7 mm apart. The heat of reaction was removed by water circulating through tubes but this being insufficient, led to localized overheating and carbon deposition over the catalyst. After a series of improvements, both at the lab scale and the industrial scale, involving the use of tubular arrangement of catalyst bed, use of recycle gas, led to the development of the reactors which were installed at Sasol in 1954. (Figure I-21). Each of these reactors has about 2052 single tubes of 46 mm ID. The length of each tube is about 12 m. The outside of the tubes is surrounded by boiling water, the temperature of which is controlled by regulating the pressure. Typical operating conditions employed are 2.7 MPa and 493 to 523 K. The use of a high gas linear velocity through the catalyst bed ensures that the heat of reaction is removed along the length of the tubes and this results in a near-isothermal reactor operation (Dry, 1981).

The design problem of a fixed bed reactor can be approached at various levels of sophistication. One dimensional models take into account variations in composition and temperature along the length of the reactor, while two-dimensional models allow for variations in these properties in the radial direction also. Models based on the assumption that the reaction takes place

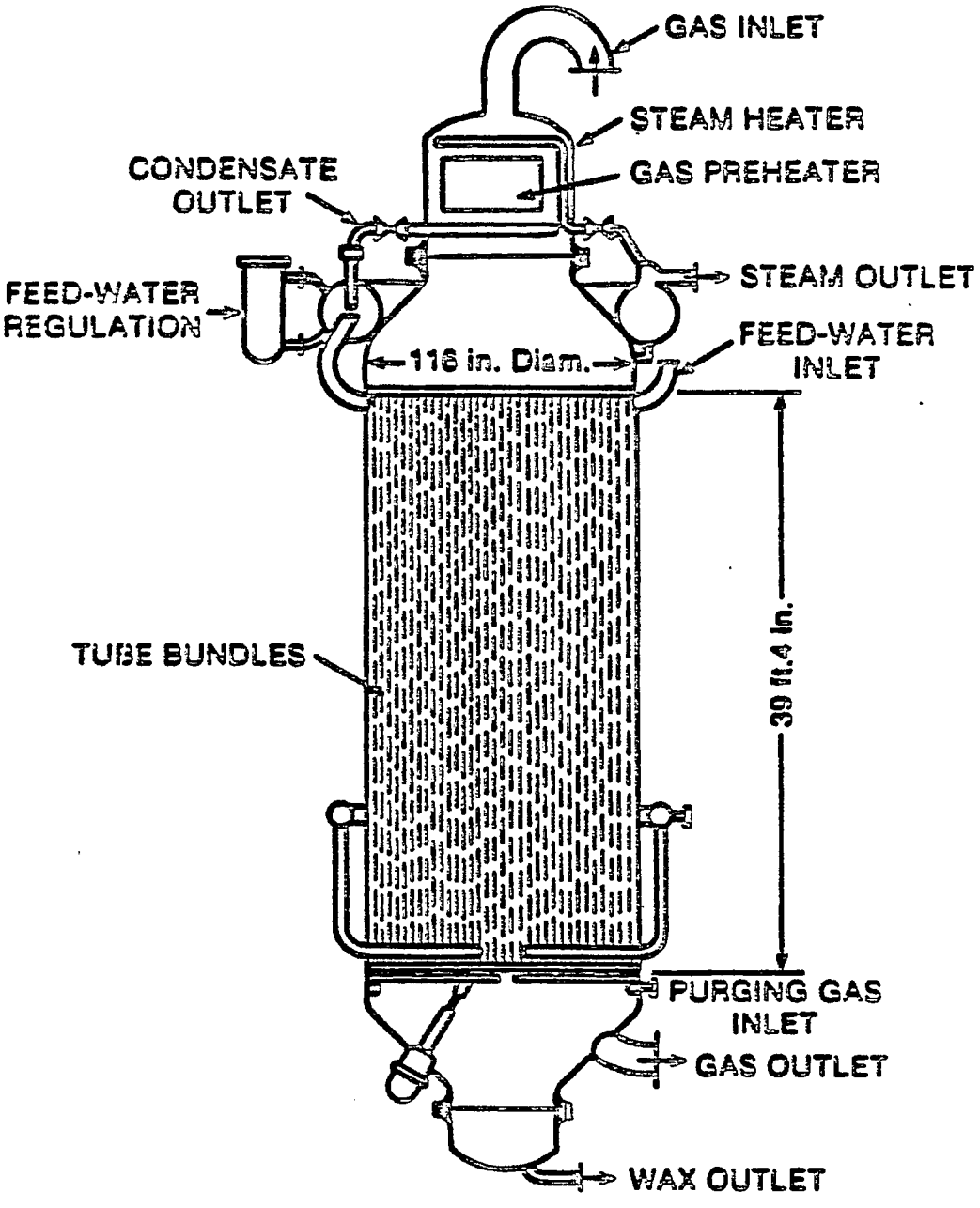

Figure I-B-21: Sasol Arge Fixed Bed Reactor

throughout the reactor volume constitute the pseudo-homogeneous model while heterogeneous models explicity account for the presence of the solid catalyst, besides the fluid.

Pseudo-homogeneous models of fixed bed reactors are widely employed in reactor design. Such models assume that the fluid within the volume element associated with a single catalyst pellet or group of pellets can be characterized by a bulk temperature, pressure and composition. In most industrial scale equipments, the reactor volume is so large compared to the volume of the individual pellet and the fraction of the void volume associated therewith that the assumption of continuity is reasonable. Much discussion has arisen as to whether intraparticle transport phenomena may play a significant role during synthesis. (Atwood and Bennet, 1979). There is some doubt on the type of diffusion occuring in the pores partially filled with liquid hydrocarbons. Since the liquid phase may be partially boiling and condensing during the reaction, and molecular diffusion could be superimposed by turbulent diffusion so that estimates using values of the diffusion coefficients for molecular diffusion will be too conservative. Furthermore, it is possible that the catalyst is only active on its outer layer because the inner part of the catalyst may be in an inactive oxidized state due to water produced. (Bub and Baerns, 1980) The model developed in the present work is based on the simplified pseudo-homogeneous model in one dimension to describe the performance of an F-T reactor with Ru/Al_2O_3 catalyst.

a. Model Assumptions:

i) The reactor is operated under steady state conditions

ii) The species concentration, fluid temperature and the pressure vary along the axial direction only

iii) Heat transfer between the cooling fluid and the reactor walls is

considered by presuming that all the resistance is contained within a thin boundary layer next to the wall.

iv) Axial dispersion of heat and mass along the tube length is neglected

v) The fluid phase is assumed to obey the ideal gas law.

vi) Pressure at various points along the bed is estimated using the Ergun's equation.

vii) The kinetic expression used is the one reported for F-T synthesis over Ru/Al_2O_3 catalyst (Stern et al., 1985b). The kinetic expression was based on data taken under negligible mass transfer limitations. It is assumed that the same conditions prevail in the fixed bed reactor, i.e. the presence of both interphase and intrapellet gradients is neglected. This assumption is certainly very restrictive and would tend to overpredict the reactor performance.

ix) The mass velocity remains constant along the reactor axis

x) Variation of physico-chemical properties such as specific heats, viscosities and heat of reaction with temperature is ignored.

xi) The resistance of heat transfer across the tube wall is assumed to be predominant on the gas side.

xii) Variation in the gas velocity due to volumetric contraction is taken into account using the concept of Levenspiel (1972).

b. Model Equations:

Component mass balance:

$$\frac{dX_i}{dz} = \frac{M_i}{G} R_i$$

$$\text{with } X_i = X_{io} \quad @\ z = 0 \tag{76}$$

where, R_i represents the net formation of component i

Hydrogen

$$R_{H_2} = -\rho_B \left[3.0\ B_1\ P_{H_2}^{a_1}\ P_{CO}^{b_1} + 5.0\ B_2\ P_{H_2}^{a_2}\ P_{CO}^{b_2} + 7.0\ B_3\ P_{H_2}^{a_3}\ P_{CO}^{b_3}\right.$$

$$\left. + B_4\ P_{H_2}^{a_4}\ P_{CO}^{b_4} \sum_4^{\infty} (2n+1)\ \alpha^{n-4}\right] \tag{77}$$

$$R_{CO} = -\rho_B \left[B_1\ P_{H_2}^{a_1}\ P_{CO}^{b_1} + 2.0\ B_2\ P_{H_2}^{a_2}\ P_{CO}^{b_2} + 3.0\ B_3\ P_{H_2}^{a_3}\ P_{CO}^{b_3} +\right.$$

$$\left. B_4\ P_{H_2}^{a_4}\ P_{CO}^{b_4} \sum_4^{\infty} n\ \alpha^{n-4}\right] \tag{78}$$

$$R_{H_2O} = -R_{CO} \tag{79}$$

$$R_{C_n} = \rho_B \left[B_n\ P_{H_2}^{a_n}\ P_{CO}^{b_n}\right] \quad \text{for } n = 1,2,3 \tag{80}$$

$$R_{C_n} = \rho_B \left[B_4\ P_{H_2}^{a_4}\ P_{CO}^{b_4}\ \alpha^{n-4}\right] \quad \text{for } n \geq 4 \tag{81}$$

$$B_n = A_n \exp\left[\frac{-En}{RT}\right]$$

Energy Balance:

$$\frac{dT}{dz} = \left[-\frac{4}{D_T} h_w (T - T_w) - R_{H_2} (-\Delta H)\right] \left(\frac{1}{GC_p}\right) \qquad (82)$$

with $T = T_o$ @ $z = 0$

Pressure Balance:

$$\frac{dP}{dz} = \frac{-f G^2}{\rho_m d_p g_c} \cdot \frac{1}{1033} \qquad (83)$$

$$P = P_o \quad @ \; z = 0$$

The mass balance equations developed here are based on the following stoichiometry:

$$nCO + (2n+1) H_2 \rightarrow C_nH_{2n+2} + nH_2O$$

The various physico chemical properties of the fluid mixture and the system parameters involved in the above equations are evaluated using suitable mixing rules and correlations available in literature. These are listed in Table I-B-5.

c. Numerical Solution:

The differential equations representing the component mass balance, (equation 76) heat balance (equation 82) and the pressure balance (equation 83) alongwith the pertinent boundary conditions constitute an initial value problem which is solved using the Runge-Kutta Verner method. Use is made of the package DVERK available through the IMS library to solve the equations.

Table I-B-5

Parameters Used in Fixed Bed Reactor Model

1. Mixture Density:

$$\rho_m = \frac{P(AMW)}{RT}$$

wherew AMW is the average molecular weight of the fluid mixture

2. Mixture Viscosity:

$$\mu_m = \frac{\Sigma_i y_i \mu_i M_i^{0.5}}{\Sigma_i y_i M_i^{0.5}}, \quad y_i = \text{mole fraction}$$

3. Mixture Thermal Conductivity:

$$K_m = \frac{\Sigma_i y_i K_i M_i^{0.5}}{\Sigma_i y_i K_i^{0.5}}$$

4. Friction Factor:
(Ergun, 1952)

$$f = \left(\frac{1-\varepsilon}{\varepsilon^3}\right) \left[1.75 + 1.50 \left(\frac{1-\varepsilon}{Re}\right)\right]$$

where, $Re = \frac{D_p G}{\mu_m}$

5. Heat Transfer Coefficient:
(Leva, 1950)

$$\frac{h_w D_T}{K_m} = 3.50 \left(\frac{d_p G}{\mu_m}\right)^{0.70} \exp\left(\frac{-4.5\, d_p}{D_T}\right)$$

Parameter Effect on Reactor Performance:

•Effect of inlet gas velocity on conversion

The conversion of synthesis gas obtainable across the reactor decreases with an increasing inlet gas velocity. The reason being primarily the decrease in the residence time of the reactants. (Fig. I-B-22). The space time yield also increases with an increase in the inlet gas velocity. (Fig. I-B-23).

•Effect of inlet H_2/CO molar ratio on conversion:

Change in the inlet H_2/CO molar ratio can be brought about either by a change in the H_2 partial pressure or by a change in the CO partial pressure at the inlet. Irrespective of the above alternatives, the syn-gas conversion increases with an increase in the inlet H_2/CO molar ratio as shown in Fig. I-B-24 and Fig. I-B-25.

COMPARISON OF REACTOR PERFORMANCE

Comparison of the performance of the various reactors used for Fischer-Tropsch synthesis has to be made on a common basis taking into consideration the operating and feed conditions. In the light of the fact that the F-T reactors viz. the slurry bed, the fluidized bed and the fixed bed are operated under varied conditions of temperature, pressure, inlet composition, and catalyst characteristics. Furthermore, the phenomena involved in each of these reactors are grossly different from each other which demarkates them from each other.

Earlier comparison of reactor performance has been made with experimental data on F-T synthesis carried out in these reactors. Data collected in pilot plant studies (Hall et al., 1952) showed that when normal sized catalysts were used (i.e. normal for the reactor type) the space time yield increased in the

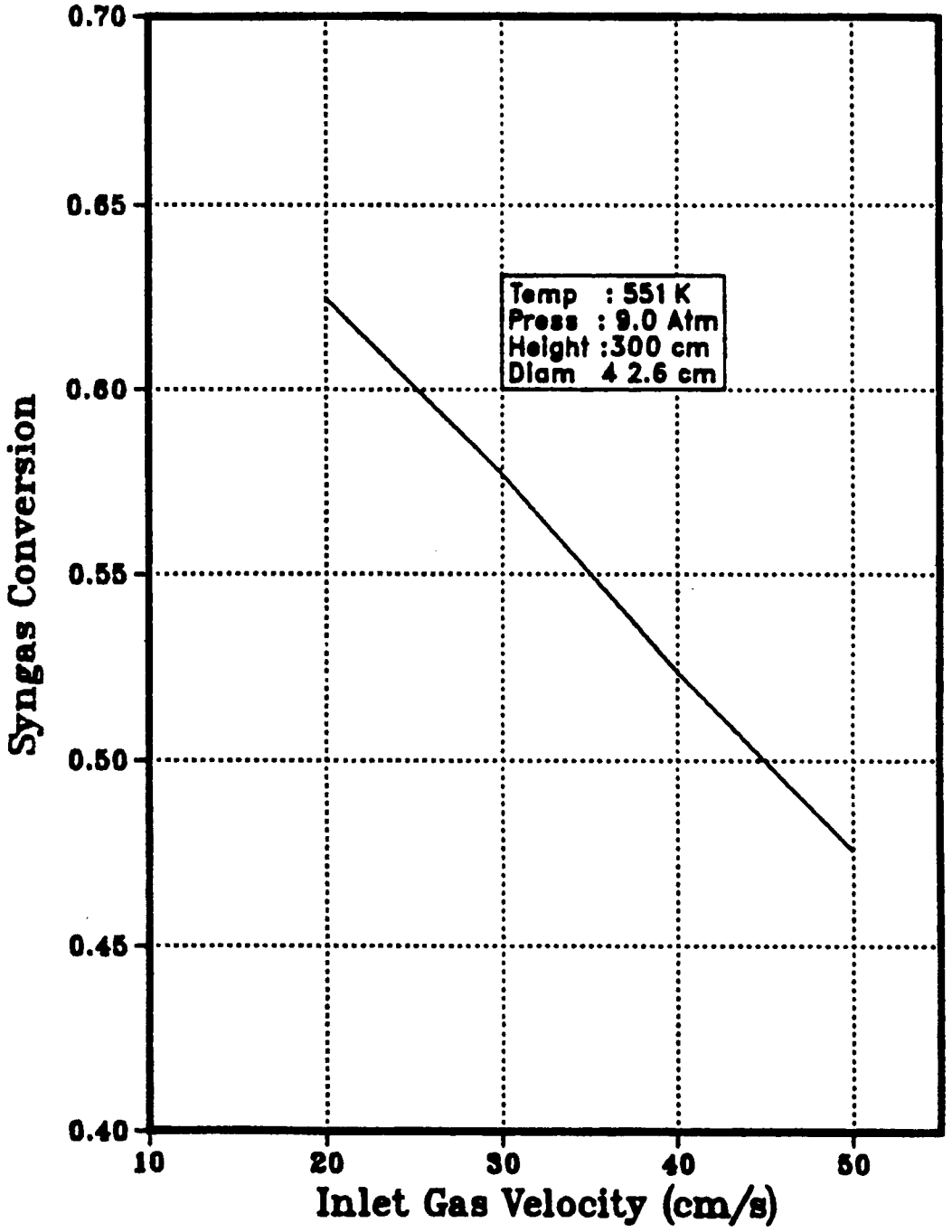

Figure I-B-22: Effect of Inlet Gas Velocity on Conversion (Fixed Bed)

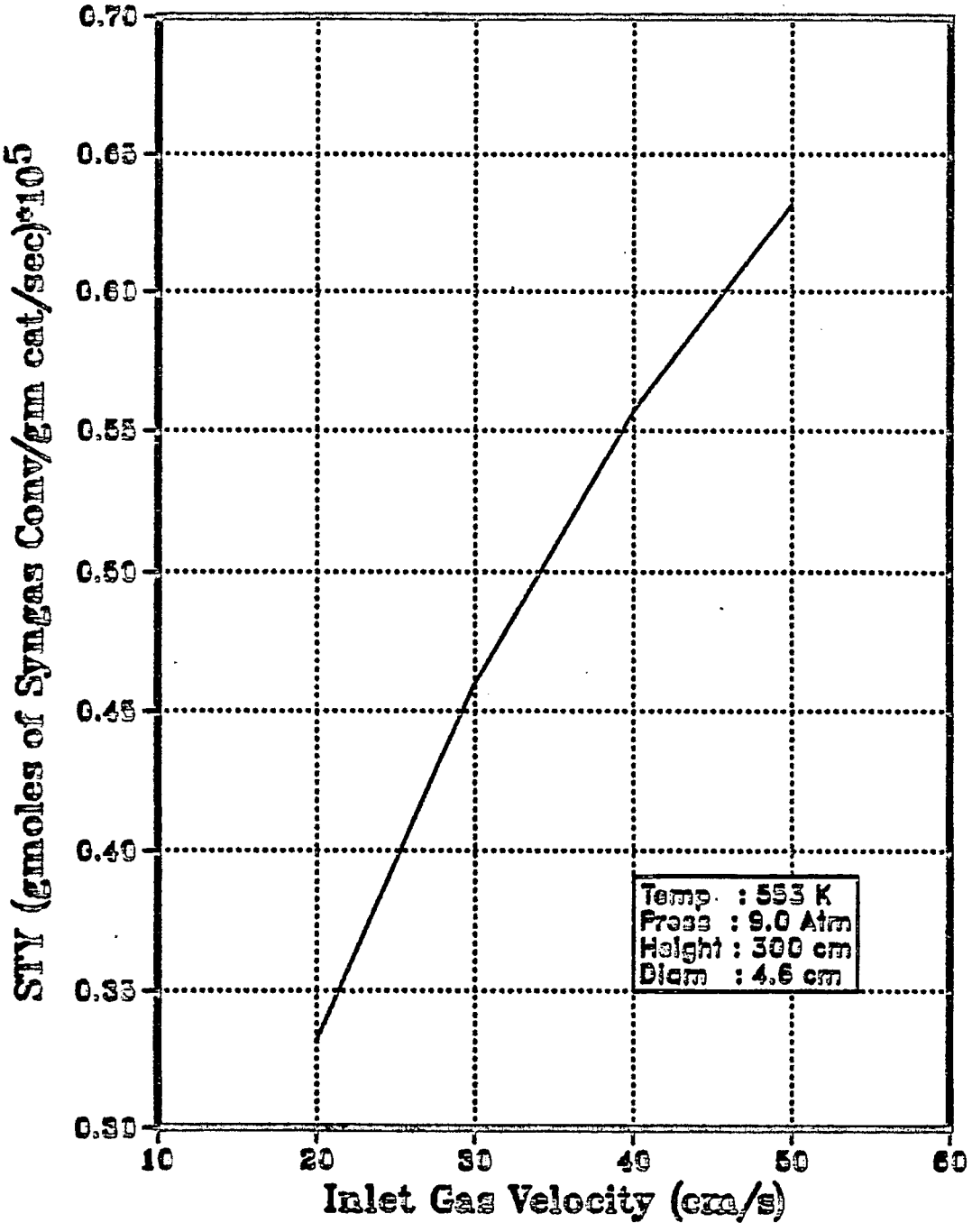

Figure I-B-23: Effect of Inlet Gas Velocity on STY (Fixed Bed)

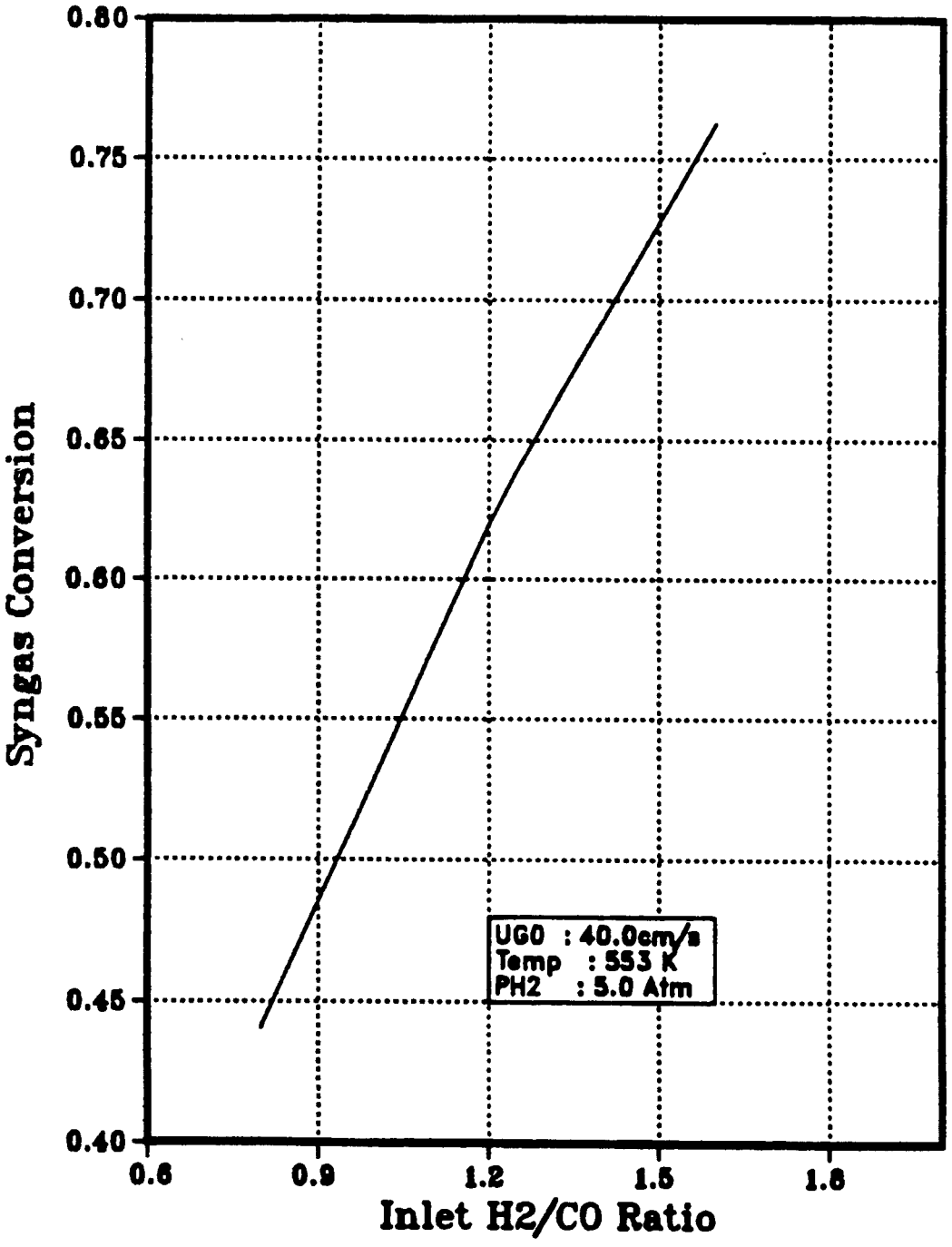

Figure I-B-24: Effect of Inlet Composition on Conversion (P_{H_2}=5)

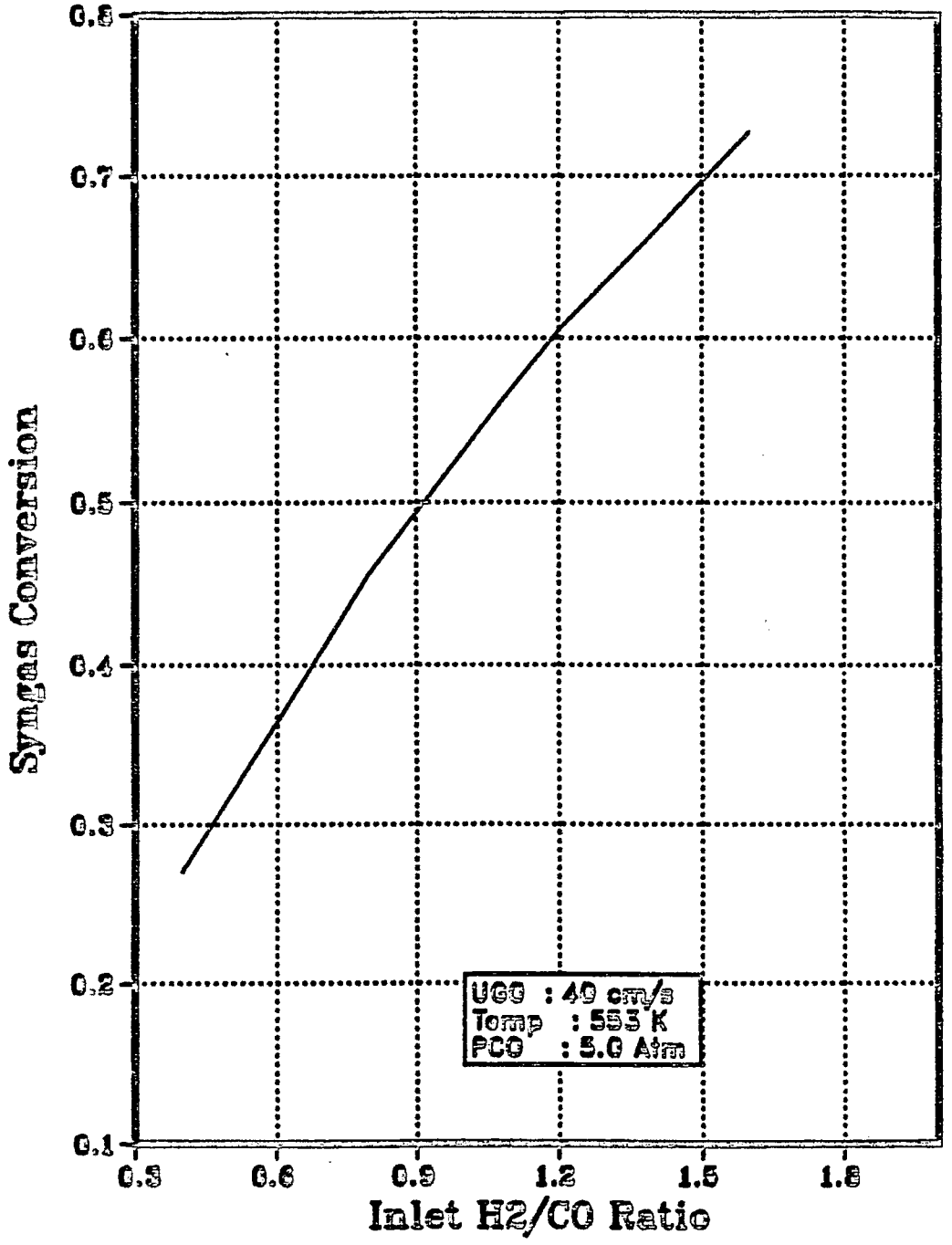

Figure I-B-25: Effect of Inlet Composition on Conversion (P_{CO}=5)

order slurry, fixed and fluidized beds. When catalysts were of the same size the order was slurry, fluidized and fixed beds. Similar studies have been carried out at the Sasol pilot plant with the commercially used catalysts (Dry, 1981). The results of the comparative tests are summarized in Table I-B-6. For each set of tests the same catalysts were used except for the particle size differences as required by the systems. Case 1 shows that under the conditions employed, the slurry bed has a somewhat higher conversion than the fixed bed reactor. The smallness of the catalyst particles in the case of slurry reactor more than compensates for the lower mass of catalyst charged. The selectivity in case of slurry bed is shifted towards the heavier products possibly due to the fact that the actual temperature of catalyst particles in the slurry bed is lower than that of the catalyst extrudates in the fixed bed. Case 2 indicates that the fluidized bed has a higher activity than the slurry bed. The bed height of the fluidized catalyst is half than that of the slurry bed but nevertheless contained four times the mass of catalyst. Increasing the catalyst charge to the slurry bed does not in practice increase the conversion as the actual gas hold-up is adversely affected. As regards the selectivities there is no discernible difference between the two reactor types. From this it may be deduced that there is little difference in the actual particle temperatures in the two reactors.

Another study directed towards the comparison of various F-T reactors, viz. slurry bed, entrained bed, tube wall, and ebullating bed reactors was carried out (Thompson et al., 1981). Although the major emphasis of this study was on a kinetic analysis of the reactor systems, to provide a theoretical explanation for intrinsic strengths and weaknesses of the reactors, a part of the study was also aimed at comparison of reactor systems

Table I-B-6

Experimental Comparison of Fixed, Slurry, and Fluidized Bed Reactors

	CASE 1		CASE 2	
	FIXED	SLURRY	FLUIDIZED	SLURRY
Catalyst Type	Precipitated		Fused	
Particle size	2.5mm	0-150μm	<70μm	<40μm
Catalyst load(kg Fe)	2.7	0.8	4.2	1.0
Bed height(m)	3.8	3.8	2.0	3.8
Bed inlet temp.(K)	496	508	593	593
Bed outlet temp.(K)	509	511	598	601
Total gas velocity (cm/sec)	36	36	45	45
%($CO+H_2$)conversion	46	49	93	79
Selectivity (% carbon atom)				
CH_4	7	5	12	12
C_3			14	14
Gasoline	14	15	43	42
Hard wax	27	31	0	0

based on physical attributes, their respective investment costs, yields, catalyst requirements, and thermal efficiencies using simplified conceptual designs.

Comparison based on space time yield and the level of conversion obtainable under a particular set of feed and operating conditions would provide meaningful insight into the respective reactor performance. In the present work, slurry bed reactor is compared with fluidized bed and fixed bed, predominantly based on this concept. In doing this, the feed composition to each of the reactors, the operating temperature and pressure are maintained the same. Thus under such conditions, the STY and the syngas conversion obtainable at the same weight hourly space velocity would indicate the relative effectiveness of a particular reactor system.

- Slury Bed Reactor vs. Fluidized bed reactor

The two reactors were compared based on the BCSR Model 1 and the FBR Model 1. It is assumed that the same catalyst is used in the two reactors and the kinetics can be represented by a first order dependence on H_2 concentration. The reactors are assumed to operate at the same temperature and pressure with the inlet gas composition also being maintained equal. Following operating conditions were assumed in the comparison.

Temperature: 546K

Pressure: 12 atm

Inlet CO/H_2 ratio: 1.5

The amount of catalyst used in the two reactors is however different, depending upon the reactor volume and their design features. Thus, the slurry bed reactor contained 800 Kg of catalyst, as against 4.2 Kg in the fluidized bed.

Comparison of reactor performance was made based on the space time yield (STY) and syngas conversion at the same weight hourly space velocity (WHSV). The two quantities viz., STY and WHSV are defined as follows:

$$STY = \frac{\text{gmoles of } H_2 \text{ converted}}{(\text{gm of catalyst})\ (\text{sec})}$$

$$WHSV = \frac{\text{gm of } H_2 \text{ fed}}{(\text{gm of catalyst})\ (\text{hr})}$$

The inlet gas velocity is varied to operate the two reactors at different WHSV; and the corresponding STY and syngas conversion obtainable from the two reactors is compared.

Fig I-B-26 shows the variation of sygas conversion with WHSV. The conversion obtained from both the reactors is equally high at low values of WHSV and gradually drops with an increase in the WHSV, due to a decreased residence time within the reactor. However, the presence of the liquid phase in the slurry reactor, introduces an additional resistance for transport, viz., the mass transfer resistance at the gas-liquid interface. Furthermore, F-T synthesis in the slurry phase being in the "absorption-with slow-reaction" regime, the resistance of gas-liquid mass transfer and the kinetic resistance are comparable. Increase in the WHSV due to an increase in the superficial gas velocity may lead us from a mass transfer controlled regime to a totally kinetic controlled regime as exhibited by a sharp decrease in conversion with WHSV. Such a phenomenon is not observed in case of a fluidized bed reactor, where the drop in conversion is more gradual and in fact the level of conversion becomes higher than the slurry bed at higher values of WHSV. The

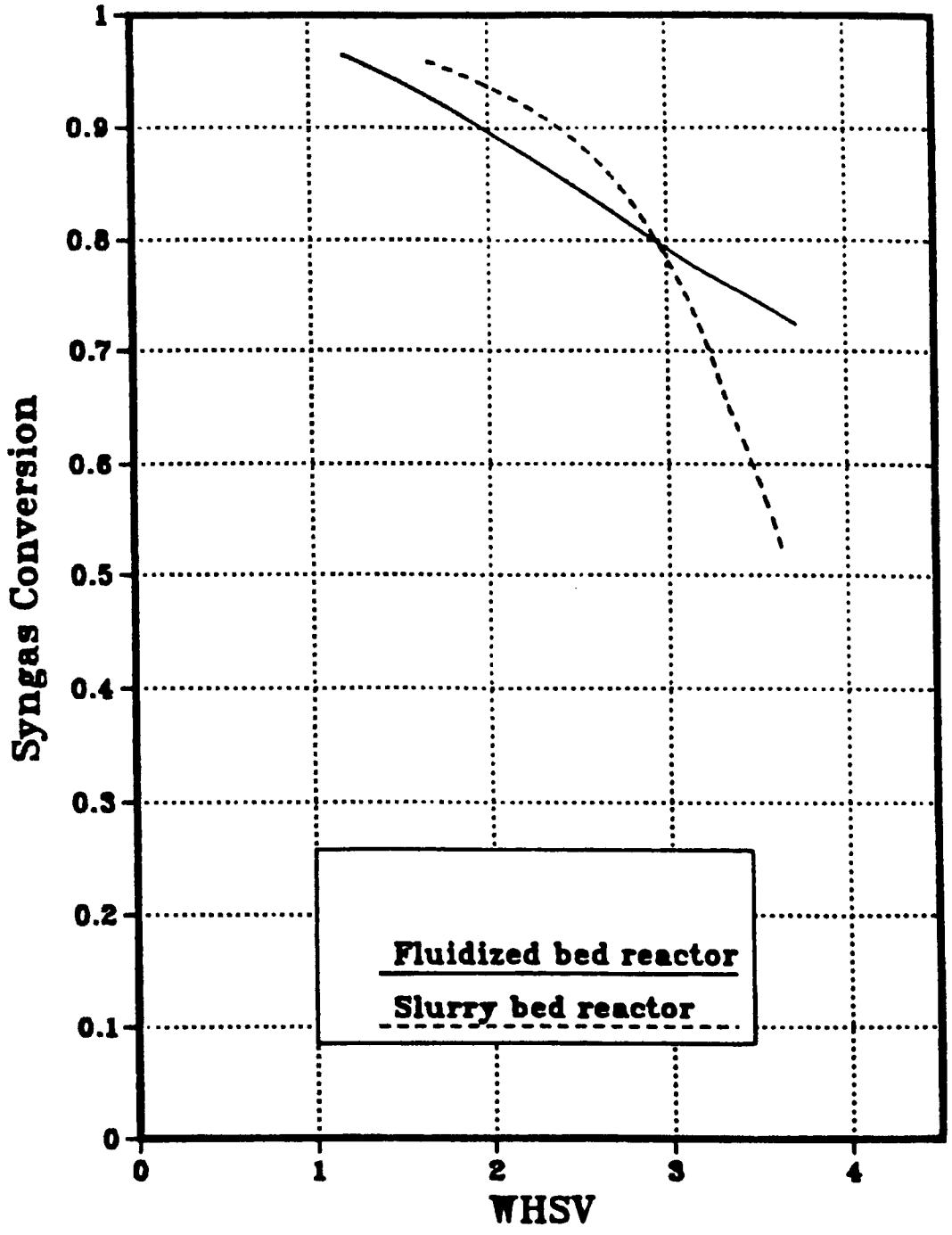

Figure I-B-26: Syngas Conversion v/s WHSV (Slurry bed and Fluidized bed)

effect of the relative resistances becomes more clear in the variation of STY with WHSV. (Fig. I-B-27). The STY in case of a BCSR shows a maxima corresponding to the optimum operating velocity, in contrast to the fluidized bed reactor, which shows an increasing profile of STY with WHSV even at higher operating velocities.

Thus based on the criteria of syngas conversion and STY, the two reactors are comparable at lower values of WHSV, but at higher valves of WHSV, the fluidized bed reactor edges over the slurry bed although the final choice would be greatly governed by the relative economics.

- Slurry bed reactor v/s Fixed bed reactor

Use is made of the BCSR MODEL 2 and the fixed bed reactor model to compare the performance of the two reactors. The criteria of STY and syngas conversion at the same WHSV is used in the comparison. It is assumed that the reactors are operated at the same temperature, pressure and feed composition. Following conditions were used in the comparison:

Temperature : 553 K

Pressure : 13 atm

Inlet H_2/CO ratio: 1.6

The operation of both the reactors was assumed isothermal. The amount of catalyst in the two reactors were as follows:

Slurry bed : 41.3 gm.

Fixed bed : 12.47Kg

The variation of syngas conversion with WHSV is as shown in Fig. I-B-28. The WHSV was varied by changing the superficial gas velocity. As seen in the

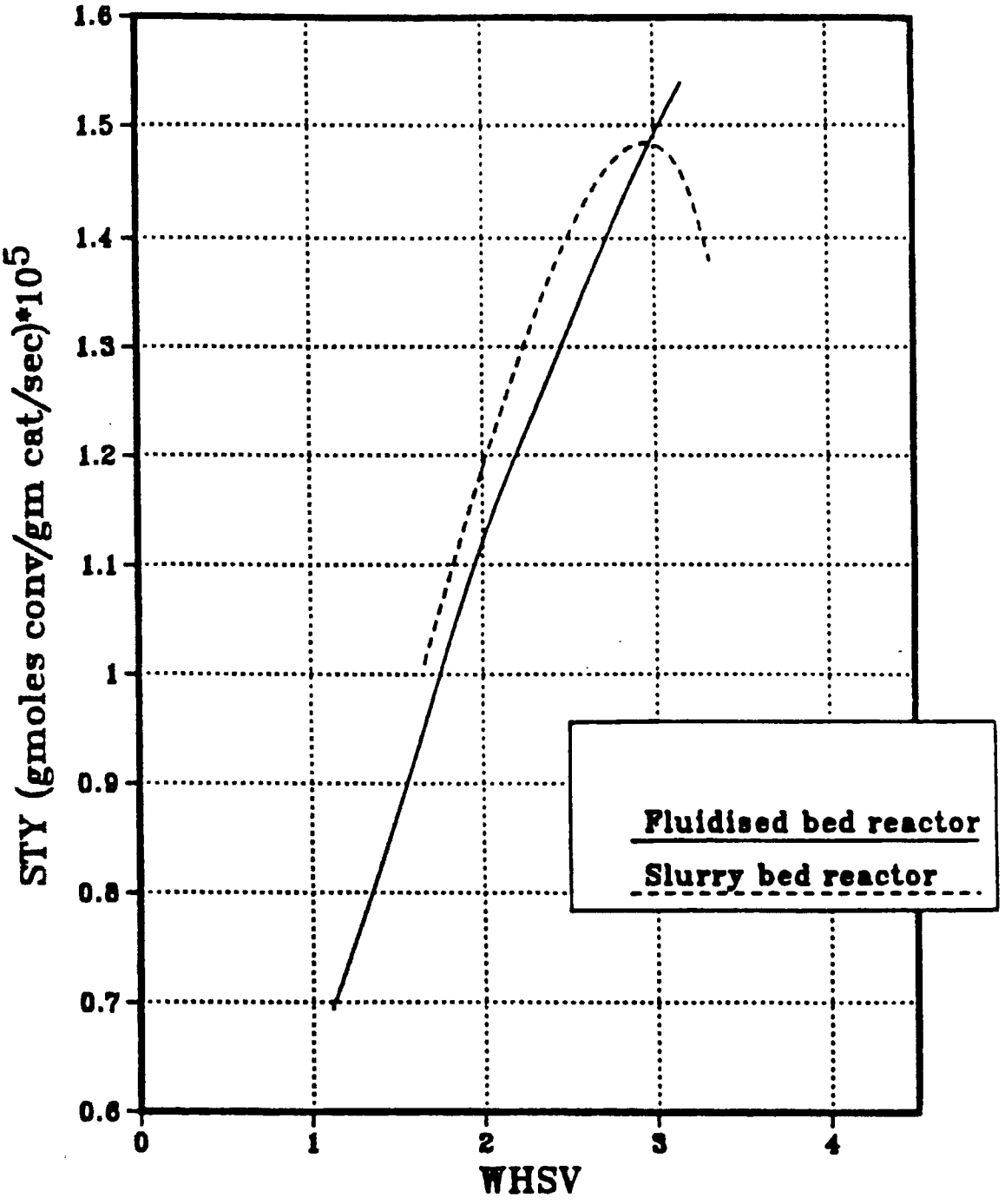

Figure I-B-27: STY v/s WHSV (Slurry bed and Fluidized bed)

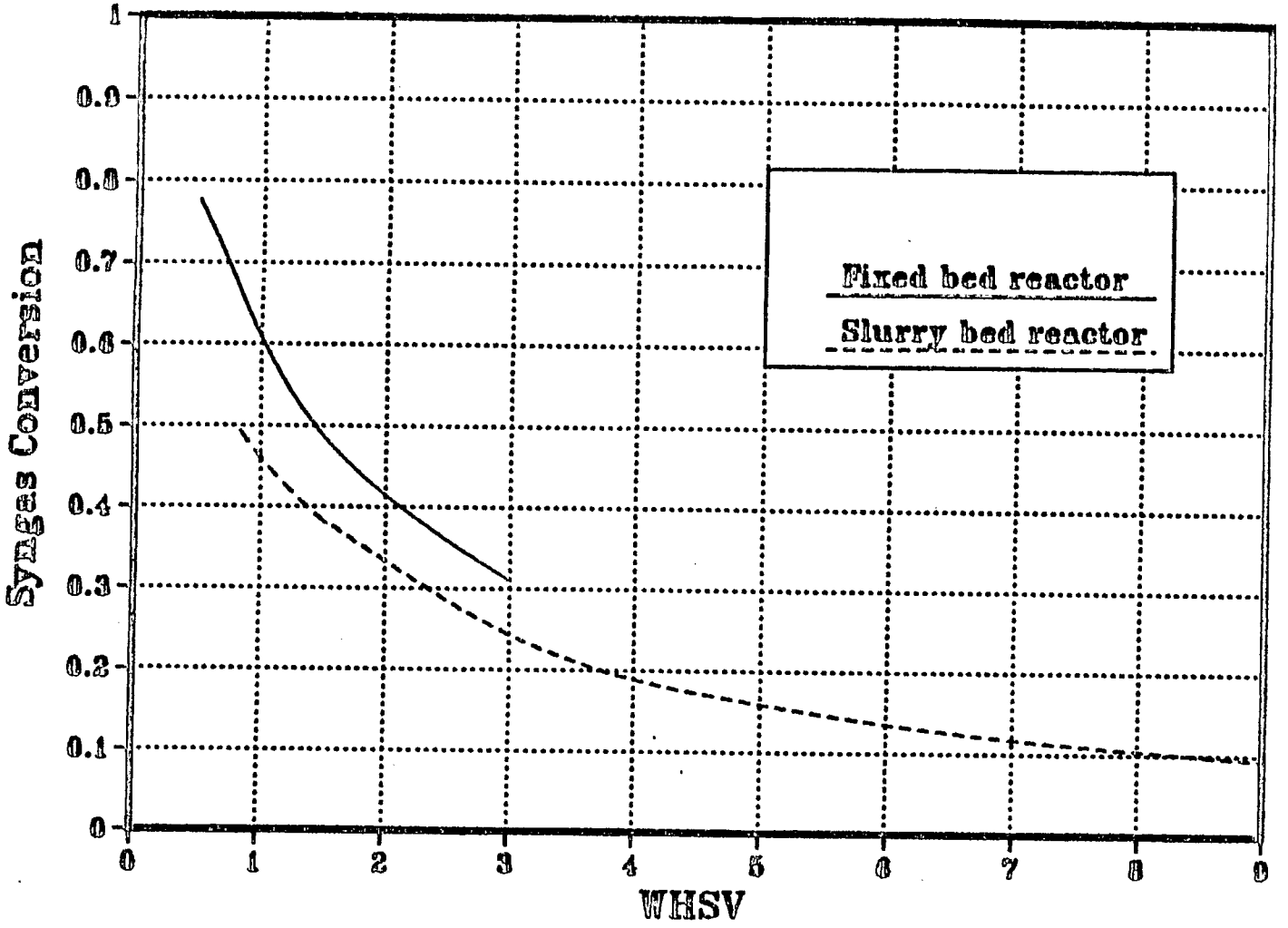

Figure I-B-28: Syngas Conversion v/s WHSV (Slurry bed and Fixed bed)

figure, the conversion obtainable in a fixed bed reactor is higher than in case of a slurry bed reactor and gradually decreases with an increase in the value of WHSV. Variation of STY with WHSV also indicates a higher STY in case of a fixed bed reactor in comparison to the slurry bed. As seen in Fig. I-B-29, the STY in case of slurry bed levels off with respect to WHSV in comparison to the fixed bed. This may be attributed to the presence of the mass-transfer resistance at the gas-liquid interface in case of the slurry reactor. Although, in the above comparison, the fixed bed may appear to be more effective than the slurry bed, but since the presence of the intra and inter phase mass transfer resistances were neglected in case of the fixed bed reactor model, the performance may have been overpredicted in its favor.

From the concentrations of the various species obtained in slurry bed and fixed bed reactor, one can evaluate the amount of products formed per unit amount of reactants consumed. The amounts of each of these species per unit amount of reactants consumed in both the reactors increases with a decrease in the superficial gas velocity. This may be attributed to the increased residence time within the reactor.

However, selectivity in case of a fixed bed reactor largely depends on various factors such as mass transfer resistances, both the intra and the inter-phase, the temperature of the catalyst pellet etc. And hence, unless these are suitably accounted for, one cannot generalize the comparison based on product selectivity. However, taking into account the complexity of the overall phenemenon of F-T synthesils in a fixed bed reactor, such an analysis would call for an extensive computation and analysis.

- Physical Comparison

  The Fischer-Tropsch section is a small part of an indirect liquefaction

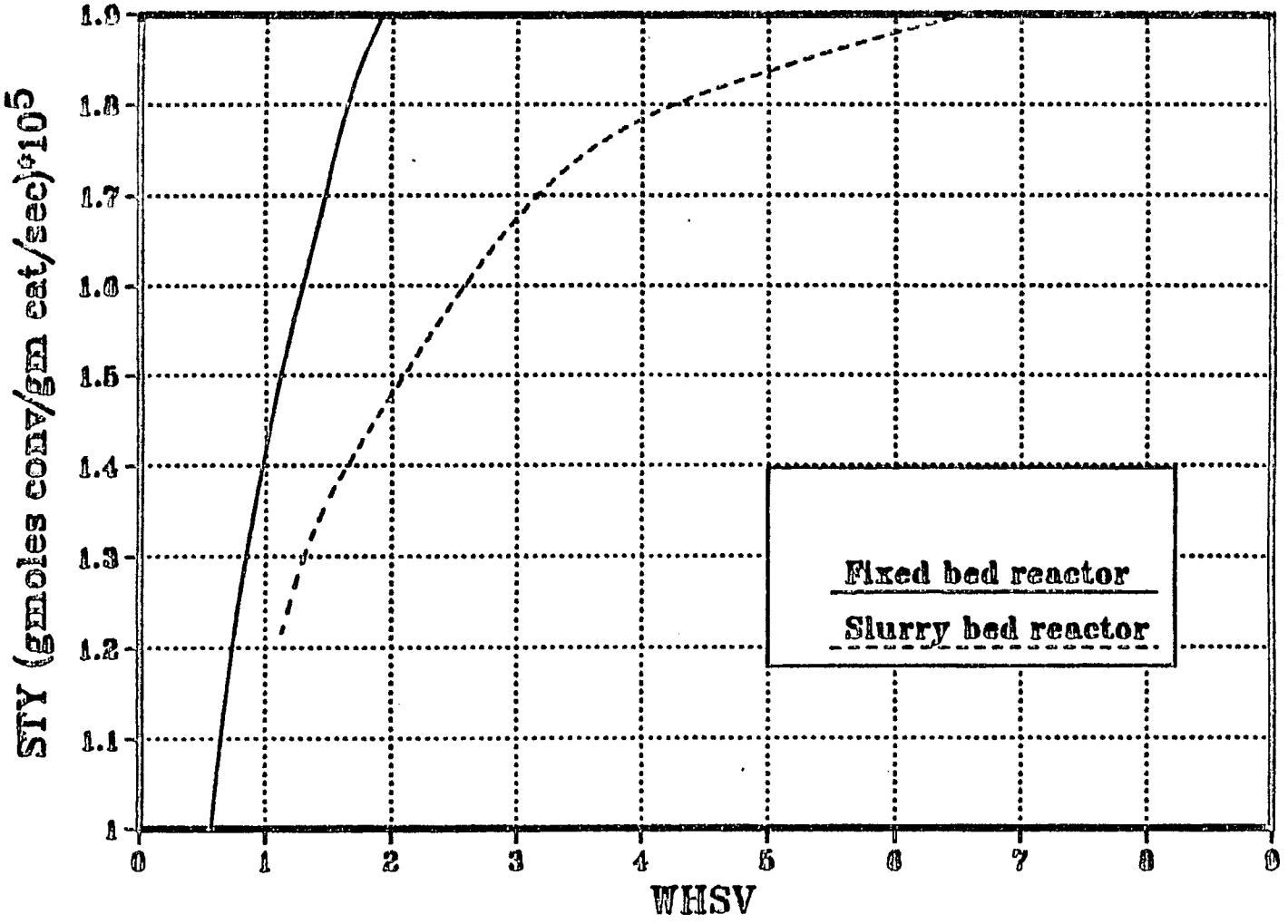

Figure I-B-29: STY v/s WHSV (Slurry bed and Fixed bed).

plant and, therefore, the most important economic consideration is that of product yield. With the objective being transportation fuel, especially gasoline, this means the ideal process should maximize gasoline production and minimize the amount of methane produced. In the case of a fluidized or an entrained bed reactor, to minimize the condensation of heavy products which lead to defluidization of the bed, the reactors are operated at higher temperatures thus giving rise to a lesser gasoline production and a higher methane formation. At these high temperatures, free carbon formation becomes a significant problem thus limiting the catalyst life and adding to the operating cost.

In contrast, a slurry reactor can be operated at a lower temperature and at conditions which produce a greater yield of gasoline. The slurry reactor operation allows very good temperature control and high thermal efficiency. Once through conversion of over 95% can be achieved with the proper choice of operating conditions. This leads to a much simplified process and a considerable cut in the recycle costs. Even the catalyst replacement costs would be considerably less than in case of the entrained and the fluidized bed.

The design of a fixed bed reactor is greatly governed by the control of temperature by the removal of the heat of reaction. Overheating of the catalyst seriously affects the product yield and enhances the side reactions, thus affecting the catalyst life. The use of recycle gas increases the operating costs not only associated with separation and purification but also with the increased pressure drop across the bed.

CONCLUSIONS

Computer programs developed to explain the performance of Fischer-Tropsch reactors can be used to make a study of the effect of different operating and design parameters on the reactor performance. However, in this parametric study, since the effect of individual parameter is studied, one cannot arrive at the optimum conditions that should be maintained.

The kinetic expressions used in the simulator, viz. a first order and a power law type model, correspond to Fischer-Tropsch synthesis over Fe or Ru catalysts,. Such expressions greatly simplify the mathematical analysis of the resulting equations, however modifications should be made to incorporate other non-linear rate expressions proposed in literature. Kinetic expressions in the form of power law as used for Ru catalyst lump the products based on the carbon numbers. Although, such an expression is useful in predicting the amounts of various products obtainable based on carbon numbers, yet it would be even instructive if kinetic expressions based on the formation of product types is used e.g. paraffins, olefins, alcohols, etc.

Besides the hydrocarbon formation reaction, which is a major reaction in F-T synthesis, the water gas shift reaction plays a vital role in the overall process. In the equations developed in the present report, the influence of water gas shift reaction was ignored. However, one can incorporate this influence by using the kinetics of water gas shift reaction. This would help in analysing the effect due to water inhibition at high syngas conversions or operating temperature.

The model equations used especially in the case of fluidized or fixed bed reactor are considerably simplified because of the assumptions on which they are based. These simplifying assumptions could be further relaxed to account for the various phenomena observed during F-T synthesis, in a greater

detail. Such an attempt is necessary if one has to predict the entire product distribution and the inter-relationship with the operating parameters. This would however call for a much involved theoretical and mathematical analysis.

Nomenclature

Ac	Area of cross-section of fluidized bed reactor, cm^2
An	Pre-exponential for hydrocarbon products containing n carbon atoms, gmol/gm sec $(atm)^{an+bn}$
Ar	Archimedes number
$\underline{a}$	Gas-liquid interfacial area per unit volume, cm^{-1}
An	Order with respect to hydrogen for the production of hydrocarbons containing n carbon atoms
$\underline{a}_{SL}$	Solid-liquid interfacial area per unit volume, cm^{-1}
b_n	Order with respect to carbon monoxide for the production of hydrocarbon containing n carbon atoms
C_{av_H}	Average concentration of H_2 in fluidized bed, gmol/cc
C_{cat}	Catalyst concentratoin in suspension, gm/cc
C_{c_i}	Concentration of component i in the cloud-wake phase, gmol/cc
C_{CH}	Hydrogen concentration in the cloud-wake phase, gmol/cc
C_{EH}	Exit concentration of H_2 in fluidized bed, gmol/cc
C_G	Total gas concentration, gmol/cc
C_{GH}	Gas phase hydrogen cocentration, gmol/cc
C_{GHO}	Inlet gas phase hydrogen concentration, gmol/cc
C^*_{GH}	Equilibrium hydrogen concentration
C_{LH}	Liquid phase hydrogen concentration, gmol/cc
C_P	Specific heat of fluid, cal/gm/c
C_{PH}	Hydrogen concentration in the particulate phase, gmol/cc
C_{P_i}	Concentration of component i in the particulate phase, gmol/cc
$\overline{C}_s$	Average solids concentration, gm/cc
C^o_s	Solids concentration at the bottom of the column, gm/cc
C_{SH}	Hydrogen concentration at catalyst surface, gmol/cc
Da_{cn}	Damkohler number for products containing n carbon atoms

D_e	Equivalent bubble diameter, cm
D_{Gi}	Gas phase dispersion coefficient of component i, cm^2/sec
D_{Li}	Liquid phase dispersion coefficient of component i, cm^2/sec
D_T	Diameter of reactor tube, cm
d_p	Particle diameter, cm
d_R	Diameter of column, cm
En	Activation energy for products containing n carbon atoms, Kcal/mol
E_S	Dispersion coefficient for solids, cm^2/sec
Fr	Froude number
F_s	Solids circulation rate, gm/sec
f	Friction factor
f_B	Void fraction of a fixed bed
fw	Ratio of wake volume to bubble volume
G	Mass velocity, $gm/cm^2/sec$
g	Gravitational acceleration, cm/sec^2
ΔH	Heat of reaction, cal/gmole
H	Height of fluidization, cm
h_w	Wall heat transfer coefficient, $cal/cm^2/sec/^\circ c$
I	Inlet CO/H_2 molar ratio
K_{BC}	Volumetric rate of gas exchange between bubble and cloud-wake per unit bubble volume, sec^{-1}
K_{CP}	Volumetric rate of gas exchange between cloud-wake and particulate phase per unit bubble volume, sec^{-1}
K_H	Rate constant for hydrogen consumption, sec^{-1}
K_i	Thermal conductivity of component i, $cal/cm/sec/^\circ c$

K_{Li}	Liquid side mass transfer coefficient for component i, cm/sec
K_m	Thermal conductivity of mixture, cal/cm/sec/°c
K_{SL}	Liquid solid mass transfer coefficient, cm/sec
L	Height of the column, cm
M_i	Molecular weight of component i
m_{cat}	Weight of catalyst, gm
m_{sus}	Weight of suspesion, gm
Ni	Stanton number for component i
n	Carbon number
P	Total reactor pressure, atm
P_{CO}	Partial pressure of carbon monoxide, atm
Pe_G	Peclet number for liquid phase
P_{H_2}	Partial pressure of hydrogen, atm
P_o	Pressure at inlet, atm
R	Gas constant
Re	Partial pressure of hydrogen, atm
R_i	Net formation of component i
γ_{cn}	Rate of formation of products containing n carbon atoms
γ_i	Rate of formation of component i, gmol/gm/sec
St_{GH}	Stanton number for hydrogen
T	Temperature, k, ^oC
T_o	Temperature at inlet, ^oC
U	CO/H_2 usage ratio
U_A	Bubble rise velocity, cm/sec
U_{cr}	Superficial gas velocity above which backmixing occurs, cm/sec

U_G	Superficial gas velocity, cm/sec
$\overline{U}_G$	Dimensionless gas velocity
U_G^o	Superficial gas velocity at inlet, cm/sec
U_{GB}	Superficial gas velocity in bubble phase, cm/sec
U_{GC}	Superficial gas velocity in cloud-wake phase, cm/sec
U_{GP}	Superficial gas velocity in particulate phase, cm/sec
U_o	Superficial gas velocity at incipient fluidization, cm/sec
U_{cs}	Settling velocity of catalyst particles in swarm, cm/sec
U_s	Solids circulation velocity, cm/sec
W_{cat}	Catalyst loading
X_{CO+H_2}	Syn-gas conversion
X_{H_2}	Conversion of hydrogen
x	Axial position
X_i	Mass fraction of component i
X_{io}	Mass fraction of component i at inlet
z	Dimensionless axial distance

Greek letters

α	Volumetric contraction factor, chain growth probability factor
ε_B	Fraction of bed volume occupied by bubbles
ε_G	Gas phase holdup
ε_L	Liquid phase holdup
ε_o	Void fraction at incipient fluidization
η	Liquid-solid mass transfer effectiveness factor
θ_{G_i}	Dimensionless gas phase conventration of component i
θ_{L_i}	Dimensionless liquid phase concentration of component i

μ_L	Viscosity of liquid, gm/cm/sec
μ_m	Viscosity of mixture, gm/cm/sec
μ_{SL}	Viscosity of slurry, gm/cm/sec
ρ_{cat}	Density of catalyst, gm/cc
ρ_m	Density of mixture, gm/cc
ρ_L	Density of liquid, gm/cc
ρ_{SL}	Density of slurry, gm/cc
Ψ_L	Volume fraction in liquid

References

Albal, R., Shah, Y.T., Carr, N., and Bell, A.T., "Mass Transfer Coefficients and Solubilities for Hydrogen and Carbon Monoxide under Fischer-Tropsch Conditions," Chem. Eng. Sci., 39, 905 (1984).

Ascher, Y., Christiansen, J., and Russell, R.D., "Collocation Software for Boundary-Value ODEs," ACM Trans. Math. Softw. 6 (1), 80-87 (1980).

Anderson, R.B., and Emmett, P.H., "Thermodynamics of the Hydrogenation of Carbon Monoxide and Related Reactions," and "Kinetics and Reaction Mechanism of the Fischer-Tropsch Synthesis," in Catalysis, Vol. IV, Chap. 1 and 3, Reinhold Publishing Corp., New York, NY (1956).

Anderson, R.B., "The Fisher-Tropsch Synthesis", Academic Press, Inc., Orlando, Florida (1984).

Anderson, R.B., "Nitrided Iron Catalysts for the Fischer-Tropsch Synthesis in the Eighties", Catal. Rev. Sci. Eng., 21, Vol. 1, 53-71 (1980).

Atwood, H.E., and Bennett, C.O., "Kinetics of Fischer-Tropsch Reaction over Iron," Ind. Eng. Chem. Proc. Des. Dev. 18 (1), 163-170 (1979).

Borghard, W.G., and Bennett, C.O., "Evaluation of Commercial Catalysts for the Fischer-Tropsch Reaction", Ind. Eng. Chem. Prod. Res. Dev., 18, 18-26, (1979).

Bub, G., and Baerns, M., "Prediction of the Performance of Catalytic Fixed Bed Reactors for Fischer-Tropsch Synthesis," Chem. Eng. Sci. 35, 348-355 (1980).

Bukur, D.B., "Some Comments on Models for Fischer-Tropsch Reaction in Slurry Bubble Column Reactors," Chem. Eng. Sci. 38, 441-446 (1983).

Calderbank, P.H., and Moo-Young, M.B., "The Continuous Phase Heat and Mass Transfer Properties of Dispersion," Chem. Eng. Sci. 16, 39-54 (1961).

Calderbank, P.H., Evans, F., Farley, R., Jepson, G., and Poll, A., "Rate Processes in the Catalysis-Slurry Fischer-Tropsch Reaction," Catalysis in Practice, Instn. Chem. Engrs., 66 (1963).

Davidson, J.F., and Harrison, D., "Fluidized Particles," Cambridge University Press, London (1963).

Deckwer, W.D., Burckhart, R., and Zoll, G., "Mixing and Mass Transfer in Tall Bubble Columns," Chem. Eng. Sci. 29, 2177-2188 (1974).

Deckwer, W.D., "Non-isobaric Bubble Columns with Variable Gas Velocity," Chem. Eng. Sci. 31, 309-317 (1976).

Deckwer, W.D., Louisi, Y., Zaidi, A., and Ralek, M., "Hydrodynamic Properties of the Fischer-Tropsch Slurry Process," Ind. Eng. Chem. Process. Des. Dev. 19, 699-708 (1980).

Deckwer, W.D., Serpemen, Y., Ralek, M., and Schmidt, B., "Modelling the Fischer-Tropsch Synthesis in the Slurry Phase," Ind. Eng. Chem. Process. Des. Dev. 20, 231-241 (1982).

Doraiswamy, L.K., Sharma, M.M., "Heterogeneous Reactions: Analysis, Examples and Reactor Design", Vol. 1, John Wiley & Sons, New York, NY (1984).

Dry, M.E., "Advances in Fischer-Tropsch Chemistry," Ind. Eng. Chem. Prod. Res. Dev. 15, 282-286 (1976).

Dry, M.E., "The Fischer-Tropsch Synthesis," in Catalysis Science and Technology," Vol. I, Chap. 4 (Anderson, J.R. and Boudart, M., Eds.), Springer-Verlag, New York, NY (1981).

Ergun, S., "Fluid Flow through Packed columns," Chem. Eng. Prog. 48 (2), 89-94 (1950).

Farley, R., and Ray, D.J., "The Design and Operation of a Pilot-Scale Plant for Hydrocarbon Synthesis in the Slurry Phase," J. Inst. Petrl. 50, No. 482, 27-46 (1964).

Fischer, F., and Tropsch, H., "The Preparation of Synthetic Oil Mixture (Synthol) from Carbon Monoxide and Hydrogen," Brennst-Chem. 4, 276-285 (1923).

Frohning, C.D., "Fischer-Tropsch Synthese," Chemie roh stoffe aus Kohle (Falbe, J., Ed.), Stuttgart: Thieme (1977).

Frohning, C.D., Kolbel, H., Ralek, M., Rottig, F., Schumr, F., and Schulz, H., "Fischer-Tropsch Process," in Chemical Feedstocks from Coal (Falbe, J., Ed., Translated by Mullen, A., Jr.), John Wiley and Sons, New York, NY (1982).

Fryer, C., and Potter, O.E., "Countercurrent Backmixing Model for Fluidized Bed Catalytic Reactors. Applicability of Simplified Solutions," Ind. Eng. Chem. Fundam. 11 (3), 338-344 (1972).

Hall, C.C., Gall, D., Smith, S.L., "Comparison of the Fixed Bed, Liquid Phase (slurry) and Fluidized Bed Techniques in the Fischer-Tropsch Synthesis", J. Inst. Petrol., 38, 845 (1952).

Hayduk, W., and Cheng, S., "Solubilities of Ethane and other Gases in Formal Paraffin Solvents," Can. J. Chem. Eng. 48, 93-99 (1970).

Hayduk, W., Castenada, R., Bromfield, H., and Perras, R., "Diffusivities of Propane in Normal Paraffin, Chlorobenzene, and Butanol Solvents," AIChE J. 19, 859 (1973).

Johnstone, H.F., Batchelor, J.D., and Shen, C.Y., "Low Temperature Oxidation of Ammonia in Fixed and Fludized Beds," AIChE Journal 1, 318-323 (1955).

Kato, Y., Nishiwaki, A., Fukuda, T., and Tanaka, S., "The Behavior of Suspended Solid Particles and Liquid in Bubble Columns," J. Chem. Eng. Jpn. 5, 112-118 (1972).

Kearns, D.L., "Fluidization Technology," Vol. 1, Hemisphere Publishing Co., Washington (1976).

Kolbel, H., and Ralek, M., "The Fischer-Tropsch Synthesis in the Liquid Phase," Catal. Rev.-Sci. Eng. 21, 225-274 (1980).

Kolbel, H., and Ralek, M., "Chemierohstoffe aus Kohle," Falbe, J., Ed., G. Thieme Verlag: Stutgart, 257 (1977).

Kunii, D., and Levenspiel, O., "Fluidization Engineering," John Wiley and Sons, New York, NY (1969).

Kuo, J.C.W., "Slurry Fischer-Tropsch/Mobil Two Stage Process of Converting Syngas to High Octane Gasoline," DOE Report, Contract No. DE-AC22-80PC 30022 (1983).

Latham, R.L., Hamilton, C., Potter, O.E., "Backmixing and Chemical Reaction in Fluidized Beds," Brit. Chem. Eng. 13, 666-671 (1968).

Leva, M., "Packed Tube Heat Transfer," Ind. Eng. Chem. 42, 2498-2501 (1950).

Levenspiel, O., "Chemical Reaction Engineering," John Wiley and Sons, New York, NY (1972).

Levenspiel, O., Baden, N., and Kulkarni, B.D., "Complex First-Order Reactions in Fluidized Reactors: Application of the KL Model", Ind. Eng. Chem. Process. Des. Dev. 17, 478-482 (1978).

Mangartz, K.H., Pilhofer, Th., "Verfahren stechnik," (Mainz) 14, 40 (1980).

Massimilla, L., and Johnstone, H.F., "Reaction Kinetics in Fluidized Beds," Chem. Eng. Sci. 16, 105-112 (1961).

Mhaskar, R.D., "Effect of Backmixing on the Performance of Bubble Column Reactors," Chem. Eng. Sci. 29, 897-905 (1974).

Mitra, A.K., and Roy, A.N., "Performance of Slurry Reactor for Fischer-Tropsch and Related Syntheses," Indian Chem. Engineer., Vol. V (3), 127-132 (1963).

Patridge, B.A., and Rowe, P.N., "Analysis of Gas Flow in a Bubbling Fluidized Bed when Cloud Formation Occurs," Trans. Instn. Chem. Engrs. (London), T349-T358 (1966).

Perry, R.H., and Chilton, C.H., "Chemical Engineer's Handbook," Mc-Graw Hill Book Co., New York, NY (1973).

Peter, S., and Weinert, M., "Uberdie Loslichkeit von H_2, CO, CO_2, und Wasserdampf in flussigen Kohlenwasserstoffen" Z. Physik. Chem. 5, 114 (1955).

Pichler, H., "Twenty-Five Years of Synthesis of Gasoline by Catalytic Conversion of Carbon Monoxide and Hydrogen," in Advan. Catal., Vol. 4, 272-341, Academic Press Inc., New York, NY (1952).

Rase,, H.F., "Chemical Reactor Design for Process Plants," J. Wiley & sons, New York, NY (1977).

Reddy, K., and Doraiswamy, L.K., "Estimating Liquid Diffusivity," Ind. Eng. Chem. Fund. 6, 77-79 (1967).

Sabatier, P., Senderens, J.B., "Nourelles Syntheses du Methane," Compt. Rend. 134, 514-516 (1902).

Sakai, T., and Kunugi, T., "Liquid Phase (Slurry) Fischer-Tropsch Synthesis," Sekiyu Gakkai Shi 17 (10), 863 (1974).

Sanger, P., and Deckwer, W.D., "Liquid Solid Mass Transfer in Aerated Suspensions," Chem. Eng. J. 22, 179-186 (1981).

Satterfield, C.N., and Huff, G.A., "Effects of Mass Transfer on Fischer-Tropsch Synthesis in Slurry Reactors," Chem. Eng. Sci. 35, 195-202 (1980).

Saxena, S.C., Rosen, M., Smith, D.N., and Reuther, J.A., "Mathematical Modelling of Fischer-Tropsch Slurry Bubble Column Reactors," submitted for publication.

Schlesinger, M.D., Benson, H.E., Murphy, E.M., and Storch, H.H., "Chemicals from Fischer-Tropsch Synthesis," Ind. Eng. Chem. 46, 1322-1326 (1954).

Stephen, G.K., Sinclair, R.J., Potter, O.E., "Gas Exchange between Bubbles and Dense Phase in a Fluidized Bed," Powder Technology 1, 157-166 (1967).

Stern, D., Bell, A.T., and Heineman, H., "A Theoretical Model for the Performance of Bubble-Column Reactors Used for Fischer-Tropsch Synthesis," Chem. Eng. Sci., 40 (9), 1665-1677 (1985a).

Stern, D., Bell, A.T., Heinemann, H., "Experimental and Theoretical Studies of Fischer-Tropsch Synthesis over Ruthenium in a Bubble Column Reactor," submitted to Chem. Eng. (1985b).

Shah, Y.T., and Deckwer, W.D., "Scaleup in the Chemical Process Industries," (Kabel, R., Bisio, A., Ed.) John Wiley & Sons, New York, N.Y. (1982)

Thompson, G.J., Riekena, M.L., Vickers, A.G., "Comparison of Fischer-Tropsch Reactor Systems. Phase I-DOE Report, Contract No. DEAC01-78ET10159, (1981).

Toomey, R.D., and Johnstone, H.F., "Gaseous Fluidiazation of Solid Particles," Chem. Eng. Prog. 48, 220-226 (1952).

Zaidi, A., Louisi, Y., Ralek, M., and Deckwer, W.D., "Mass Transfer in the Liquid Phase Fischer-Tropsch Synthesis," Ger. Chem. Eng. 2, 94 (1979).

Page Intentionally Left Blank